DEVELOPING PAVEMENT SAFETY BASED GUIDELINES FOR IMPROVING HORIZONTAL CURVE SAFETY

A Thesis

by

YASH MENARIA

Submitted to the Office of Graduate and Professional Studies of
Texas A&M University
in partial fulfillment of the requirements for the degree of

MASTER OF SCIENCE

Chair of Committee,	Dallas N. Little
Co-Chair of Committee,	Jon Epps
Committee Member,	Bruce Herbert
Head of Department,	Robin Autenrieth

August 2018

Major Subject: Civil Engineering

ABSTRACT

Inadequate skid resistance on wet pavements, specifically on horizontal curves of rural highways, is responsible for vehicle crashes and fatalities. Several research projects have developed models that project the effect of various geometric and pavement parameters on skid resistance. This study is an attempt to revise an existing model proposed by Texas A&M Transportation Institute (TTI) researchers. The proposed model is based on pavement parameters including (mix type, gradation, aggregate parameters and traffic parameters).

Laboratory and field tests (circular track meter (CTM), dynamic friction tester (DFT), 3-wheel polisher, micro-deval test, aggregate image measuring system (AIMS) and skid trailer test) were conducted on various treatment sites, aggregate types and mix types to analyze their performance and effects on skid resistance. Data used for this study include the data collected from laboratory and field tests, data from TxDOT pavement management information system (PMIS) along with data from past research. This study is a contribution to revise some equations in an existing skid prediction model and to develop a database consisting of skid related data which would help practitioners in taking pavement-safety related decisions on horizontal curves.

DEDICATION

I dedicate this thesis to my wonderful family, for their unconditional love and support.

ACKNOWLEDGEMENTS

I would like to thank my supervisor, Mr. Bryan Wilson, for the patient guidance, encouragement, supervision and support throughout my master's degree that enabled me to develop better understanding of the subject. I have been very lucky to have a supervisor who cared so much about my work and responded to my queries promptly.

My sincere thanks to my committee chair, Dr. Little, committee co-chair, Dr. Epps and committee member, Dr. Herbert for their guidance and support throughout the course of this research.

I would like to express my gratitude to Dr. Tom Scarpas for his valuable insights in the project. This thesis would not have been possible without the cooperation and support by Mr. Arif Chowdhury, Mr. Mike Pratt, Mr. Srinivas Geedipally, Mr. Subasish Das and Mr. Pawan Dixit.

I would also like to acknowledge my friends, colleagues and department faculty and staff for an amazing experience and lots of memories in Texas A&M University.

Finally, I must express my profound gratitude to my parents, especially my father for providing me continuous motivation and support throughout my years of study. This accomplishment would not have been possible without him.

CONTRIBUTORS AND FUNDING SOURCES

This work was supervised by my thesis committee consisting of Professor Dallas Little (committee chair), Professor Jon Epps (committee co-chair) from Department of Civil Engineering, TAMU and Professor Bruce Herbert (committee member) from Department of Geology and Geophysics, TAMU.

Funding Sources

Graduate study was supported by a fellowship from Texas A&M University and a thesis research fellowship offered by my supervisor, Mr. Bryan Wilson (Associate Research Scientist at Texas A&M Transportation Institute) and funded by the Texas Department of Transportation.

TABLE OF CONTENTS

Page

Page

LIST OF FIGURES

Page

Page

Page

LIST OF TABLES

Page

1. INTRODUCTION

1.1 Problem Statement

Horizontal curves are one of the most vulnerable roadway geometric sections for crashes on a highway system. The reasons for this include improper roadway designs, driver distraction, driving over the design speeds and insufficient skid resistance from the surface of a pavement especially in wet weather conditions. Some of the potential pavement countermeasures to reduce the crash frequency on curves including high friction surface treatments, thin overlays, seal coats, water blasting and permeable friction course. The judicious selection of a pavement surface treatment can reduce crashes and improve driver performance. This treatment has a relatively low cost compared to geometric and traffic treatments like curve straightening, increasing superelevation and implementing control-devices.

Past research studies have shown that skid resistance of a pavement is greatly affected by macrotexture (asperities of a pavement) and microtexture (harshness on the surface of aggregate). There is also a need to establish guidelines and develop a framework for practitioners to choose the appropriate treatment for a given situation. This study involves developing a database including the aggregate data, mix data, pavement types and traffic level (polishing cycles). It also focuses on revising and modifying an existing skid prediction model.

1.2 Objectives

The objectives of this study are as follows:

1. Study the effects of aggregate type and mix type on skid resistance of a pavement

2. Revise and modify an existing skid prediction model's aggregate shape characteristic equation

3. Develop a database that organizes skid-related data collected from past research, current research and the TxDOT pavement management information system (PMIS)

1.3 Thesis Organization

The thesis is organized in five main sections. The first section introduces the problem statement, objective and thesis outline. The second section contains a literature review that emphasizes pavement-safety based past research studies such as horizontal curve crashes and their influential factors, pavement treatments, performance of pavement-safety treatments and friction mechanism. The third section describes laboratory and field tests that were conducted in this study and the procedure to collect skid data and weather data. The fourth section presents data analysis and the results obtained from lab and field tests, data collected from past research and TxDOT Pavement Management Information System (PMIS). The last section discusses conclusions and recommendations of this study.

2. LITERATURE REVIEW

2.1 Overview

This section introduces the significance of horizontal curve crashes and the factors causing the crashes. In addition, it discusses crash modification factor (CMF) which is a quantity that reflects the effect of influential crash causing factors in the form of models. This section also describes pavement treatments and their performance followed by a discussion on friction mechanism.

2.2 Horizontal Curve Crashes and Influential Factors

Curves are susceptible to crashes due to many factors which affect the safety. Road safety is a major concern for any transportation agency that needs to be addressed. Twenty five percent of fatal crashes occur on horizontal curves which account for around 10,000 deaths per year (FHWA, 2011; NHTSA. 2009. "Traffic Safety Facts, 2009). Minnesota DOT analyzed crash data for 20 years and found that horizontal curves are primary hotspots for crashes on a roadway network. Horizontal curves in Minnesota accounts for about 10 percent of the state's roadway network but more than 40 percent of the severe roadway departure crashes occur on them (FHWA, 2011). It has been observed that a significantly larger portion of fatal crashes have occurred on curves with rural two-lane roadway across the nation (FHWA, 2011). More than 65 percent of the fatal crashes occurred particularly on rural two-lane highways (see Figure 1) and similar results were observed by other researchers (Schneider, 2009; Torbic et al., 2004).

2.2.1 Focus on run-off-road (ROR) crashes

Amongst the different types of collisions, the most frequent were found to be single-vehicle run off road (SVROR) and head-on (HO) crashes which accounts for 76 percent and 11 percent respectively on all roads (Torbic et al., 2004). It is essential to evaluate all the existing curves on rural two-lane highways in Texas by analyzing their crash data and come up with some effective geometric and pavement countermeasures or treatments. Texas has over 150,000 centerline miles of two-lane highways (FHWA, 2014a; Fitzpatrick, 2002).

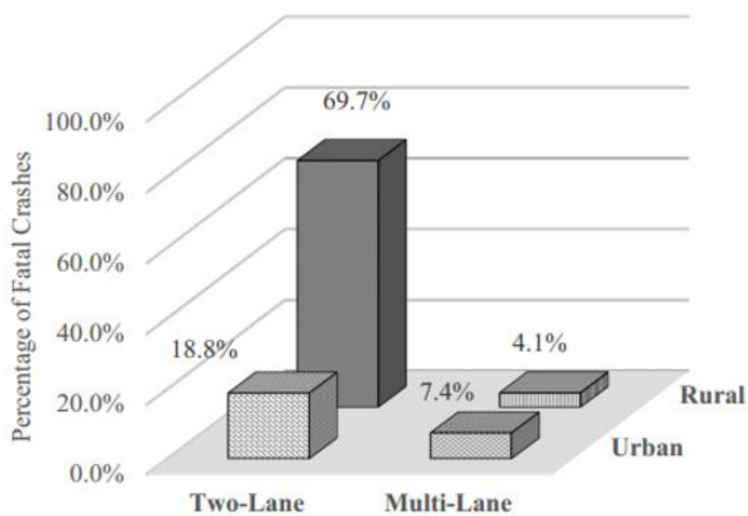

Figure 1: Percentage of fatal-crashes by roadway type (Torbic et al., 2004)

Reprinted from (Torbic et al., 2004)

2.2.2 Discussion of the Crash Modification Factor

A crash modification factor (CMF) is a dimensionless quantity that determines the effectiveness of a safety treatment based on number of crashes. It is multiplied with the expected number of crashes without treatment to analyze the expected number of crashes with treatment (FHWA, 2014). For example, a CMF lower than 1 denotes that the treatment can reduce the crashes and a CMF greater than 1 denotes that the treatment can increase the crashes. Past research studies have proposed different models for CMF which reflects the crucial factors like curve radii, design speed, deflection angles, length of a curve, radius of curvature etc. American Association of State Highway and Transportation Officials (AASHTO, 2010) in its first edition of Highway Safety Manual (HSM) has included a CMF equation which is a function of radius, length of curve and the absence of spiral transition and is given as:

$$CMF = \frac{1.55 \times Lc + \frac{80.2}{R} - 0.012 \times S}{1.55 \times Lc} \tag{1}$$

where,

CMF= crash modification factor for a horizontal curve on two-lane roadway

R= radius of curvature, ft

S= factor for spiral curve (1 if present;0 if absent)

The correlation between the radius (specially less than 1000 ft) and CMF for a 0.1-mile stretch can be seen in the Figure 2.

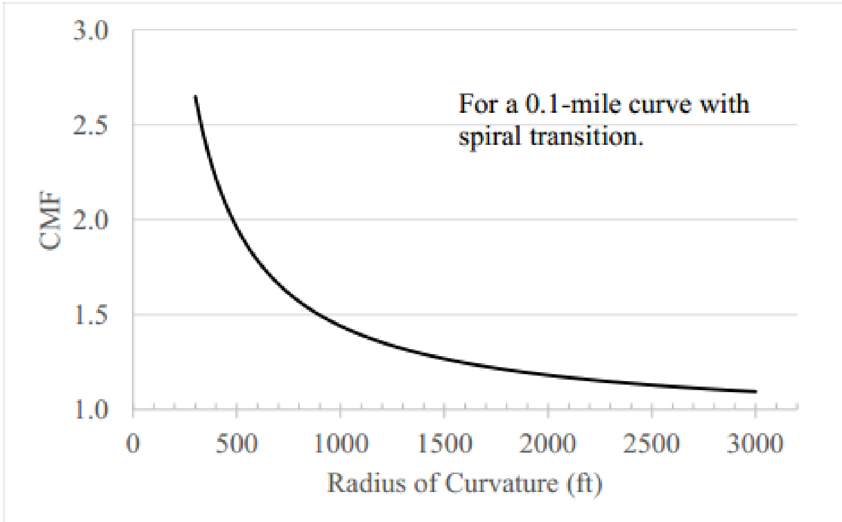

Figure 2: Relation between CMF and Radius of curvature (ft) (AASHTO, 2010)

Reprinted from (AASHTO, 2010)

Various studies have suggested CMF functions in which curve radius is one of the most common risk factor. Bonneson proposed a calibrated CMF function (Bonneson, 2008):

$$CMF_R = 1.0 + 0.106\left(\frac{5730}{R}\right)^2 \quad (2)$$

R= Radius of curvature, ft

Some studies focused on the implementation of chevrons on untreated curves and performed a before-after safety analysis. Researchers suggested the implementation of curve delineation with a CMF value 0.86 (Srinivasan et al., 2009) while (Choi, Kho, Lee, & Kim, 2015) also performed a before and after analysis on few freeways in Korea and suggested CMF for Chevrons to be 0.72. A CMF of 0.74 was estimated in a study for the evaluation of the effects of edge line markings along horizontal curves on rural-two lane highway (A. R. Tsyganov, Machemehl, & Warrenchuk, 2009).

2.2.3 Influential Factors Causing Crashes

A recent study analyzed eight year of crash data in Pennsylvania using propensity score and concluded that degree of curvature is the most significant variable to affect crash frequency (Gooch, 2016). Most of the studies use curve radii as one of the parameters and is a very crucial factor affecting safety on roadway curves. The probability of occurrence of a crash on a curve with radius less than or equal to 500 ft is double the probability of occurrence of crash on a tangent (Schneider, 2009). Zeeger also mentioned that increased crash frequency is significantly correlated with the radius or sharpness of a curve (Zegeer, 1991).

Researchers have provided two possible reasons for crashes on curves: firstly, the vehicle drivers may not be able to recognize the coming horizontal curve and secondly, they may not be able to predict the sharpness of the curve (M. P. Pratt, and J. A. Bonneson, 2008). Severity of injury can also be a significant parameter in evaluating SVROR crashes on two-lane highway horizontal curves. A study conducted in Texas (Schneider, 2009) found that the injury crashes had high probability of occurrence with the curves of radii more than 500 ft but less than 2800 ft (Schneider, 2009). SVROR crashes are fatal as the vehicles run-off from the road and hit roadside objects that result in impairment and fatalities. Some researchers performed an extensive sensitivity analysis and concluded that crash prediction is a function of annual average daily traffic

(AADT), radius and length of a curve (Findley, 2012). AASHTO in its book, *A Policy on Geometric Design of Highways and Streets* regulated the design of horizontal curves based on maximum superelevation, maximum side friction factor and the design speed (AASHTO, 2011):

$$R_{min} = \frac{V^2}{15 \times (0.01e_{max} + f_{max})} \tag{3}$$

R_{min} = minimum radius, ft

V = design speed, mph

e_{max} = maximum superelevation, %

f_{max} = maximum side friction factor

Several states department of transportation (DOT) research institutions have been consistently looking for effective counter measures to reduce crashes on horizontal curves. Walden elaborated the work plan to account for the countermeasures in his report *Developing Methodology for Identifying, Evaluating, and Prioritizing Systemic Improvements* (Walden, 2014). The study analyzed more than 6000 crashes recorded from more than 38000 curves during the year 2010-2014. More than 80 percent of the crashes were ROR (run-off road) and HO (head-on) collision was 6.5 percent (Walden, 2014). The causal factors considered in (Walden, 2014) study were curve radius, lane width, truck percentage, deflection angle and width of right shoulder. These mentioned risk factors were evaluated based on average daily traffic (ADT) and following observations were made by (Walden, 2014) as shown in Table 1.

Table 1: Effect of Risk Factors based on Traffic Levels (Walden, 2014)

Reprinted from (Walden, 2014)

Risk Factor	**Traffic level based on ADT**	**Observations**
Lane width	low traffic (ADT≤500)	more than 50 percent ROR and HO crashes on narrow lane widths (10 ft)
Right shoulder width	all traffic levels	significant increase in crashes for shoulder width < 6 ft
Truck percentage	all traffic levels	truck percentage less than 15 percent accounts for slightly increased traffic
Curve radius	all traffic levels	increased ROR and HO crashes on curves with radius ranging between 500 to 1500 ft
Deflection angle	all traffic levels	increased ROR and HO crashes for deflection angle less than 40 degrees

Curve radius represents the radius of circular arc of a curve that approximates the sharpness of the curve. If the deflection angle is less, the sharpness of a curve will be more. The deflection angle is the angle measured from tangent of point of curve (PC) or point of tangent (PT) to any other point on a curve. Lord et al. investigated some risk factors like curve geometry and its presence, weather etc. and established that the crashes on horizontal curves are significantly related to the curves with smaller radii and existence of a curve (Lord, Brewer, Fitzpatrick, Geedipally, & Peng, 2011). Their study also concluded that fatality and injury related crashes (per million vehicle miles) on horizontal curves in Texas are 2.3 per million vehicle miles more than the crashes on tangent roadway segments.

A study conducted by Long et al., 2014 used a Crash rate ratio-Skid number (CRR-SN) relationship and showed that the crash risk increases significantly with the decrease in skid number (Long, Wu, Zhang, & Murphy, 2014). Their study also suggested skid number ranges (see Figure 3 and Table 2) for all weather crashes and wet weather crashes to select countermeasures and guide practitioners at the network-level. Table 2 showed the recommended threshold levels of skid number for all weather crashes and wet weather crashes.

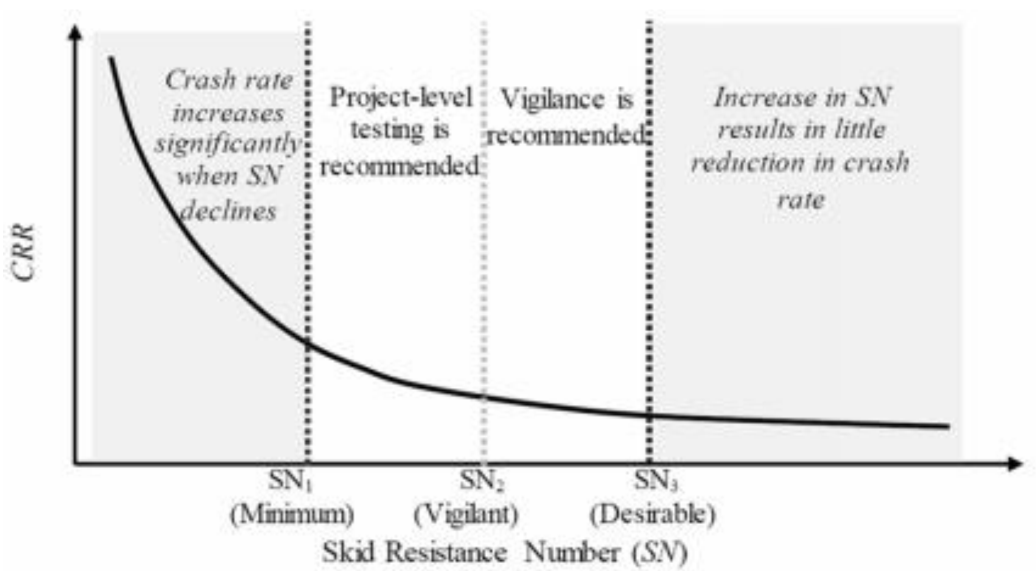

Figure 3: Schematic Diagram for Levels of Skid Numbers (Long et al., 2014)

Reprinted from (Long et al., 2014)

Table 2: Suggested threshold levels of skid number (Long et al., 2014)

Reprinted from (Long et al., 2014)

Skid Resistance Level	Suggested Threshold Values	
	All weather crashes	Wet weather crashes
SN-1	14	17
SN-2	28	29
SN-3	74	74

Researchers have also found that wet-weather related crashes are two to three times higher than on dry-pavement (Satterthwaite, 1976). Neuman et al. observed driver behavior while investigating free-flow speeds along horizontal curves on two-lane highway section in New York (Neuman et al., 2003). They concluded that drivers did not slow down enough on wet curves as they might have not recognized that the skid resistance is lower on wet pavements as compared to dry pavements.

2.3 Crash Countermeasures: Pavement and Geometric Perspective

Safety improvements suggested by various agencies like FHWA, NCHRP etc. are discussed in the Table 3.

Table 3: Performance of countermeasures in terms of CMF, cost and service life

Countermeasures	Crash type	CMF	App. Cost	Service life (yr.)	Source
Centerline markings	All (injury)	0.99	$650 per mi	2	(Elvik, 2004)
Edgeline markings	All (injury)	0.73	$650 per mi	2	(A. R. Tsyganov, R. B. Machemehl, and N. Warrenchuk, 2009)
Post-mounted delineators	All (injury)	0.70	$3000 per curve	2	TxDOT's HSIP work code
Horizontal alignment signs	All (injury)	0.82	$300 per unit	6	(McGee, 2006)
Combination horizontal alignment/advisory speed signs	All (injury)	0.87	$300 per unit	6	(Elvik, 2004)
Chevrons	SVROR	0.86	$3000 per curve	10	(Srinivasan et al., 2009)
RPM (raised pavement marking)	All (injury)	1.43	$1360 per mile	3	(Bahar, 2004)
Safety-treat fixed objects	SVROR	0.50	$300,000 per mi	20	TxDOT's HSIP work code
Dynamic curve warning system	All (injury)	0.59	$18,000 per unit	10	(McGee, 2006)
Speed advisory marking in lane	All (injury)	0.94	$300 per unit	2	(Campbell et al., 2012)
Rumble strips	SVROR+ HO	0.61	$2640 per mile	10	(Torbic D. J., 2009)
Flatten side slope	SVROR	0.54	$300,000 per mi	20	TxDOT's HSIP work code
HFST (high friction surface treatment)	All (injury)	0.55	$20/sq.yd	5	
Superelevation	All (injury)	0.35	$200,000 per mi	10	TxDOT's HSIP work code

Table 4: Crash Reduction Performance for Various Pavement Treatments

Treatment Type	Section Type	Crash Type	Approximate CMF[1]	
			Average	Range
HFST	Curves and ramps, generally high-accident locations	Wet	0.34	0.14 – 0.48
		Total	0.72	0.65 – 0.75
Seal coats	Two-way and multi-lane roads (not high-accident specific)	Wet	0.76	0.42 – 1.60
		Total	1.15	0.83 – 1.52
Thin asphalt overlays	Multi lane roads and freeways	Wet	0.87	0.53 – 1.27
		Total	0.99	0.93 – 1.20
Permeable friction course	Freeways (California and North Carolina)	Wet	0.68	0.51 – 1.04
		Total	0.94	0.74 – 1.10
Abrading and texturing	California freeways	Wet	2.03	-
		Total	0.77	-
Water blasting	-	-	-	-

1 – Crash modification factor (CMF) = 1 – Crash Reduction Factor (CRF)/100

'-' Not available

Table 4 provides a summary of CMFs for various pavement treatments. Most of these values are derived from statistically powerful studies, considering hundreds or thousands of miles of pavement, and comparing against appropriate reference sections. The CMFs for HFST, however, were obtained from far fewer study locations, and it was difficult to identify good reference sections. The data for abrading and texturing also did not have a significantly large sample size.

Pavement related countermeasures have the potential to improve the skid resistance of the road which will benefit driver performance and can result in the reduction of considerable number of crashes. Performance of pavement for curve safety can be evaluated based on its physical condition (e.g. surface distresses), functional performance (e.g. skid resistance), or ride quality assessment by the user itself. The performance indicators are rated by monitors and are given a certain rating scale. Pavement performance indicators often have threshold values to restrict further damage. Certain treatments based on the analysis are evaluated and are implemented as an immediate or long-term treatment depending on cost and service life required. Figure 4 shows that an immediate improvement was applied in the first year, pavement degraded over time and reached to its threshold. Based on pavement condition assessment, another treatment was decided which lasted from 15 years to a certain period where it again would reach to its threshold. Service life is the time until the pavement performance would return to its threshold.

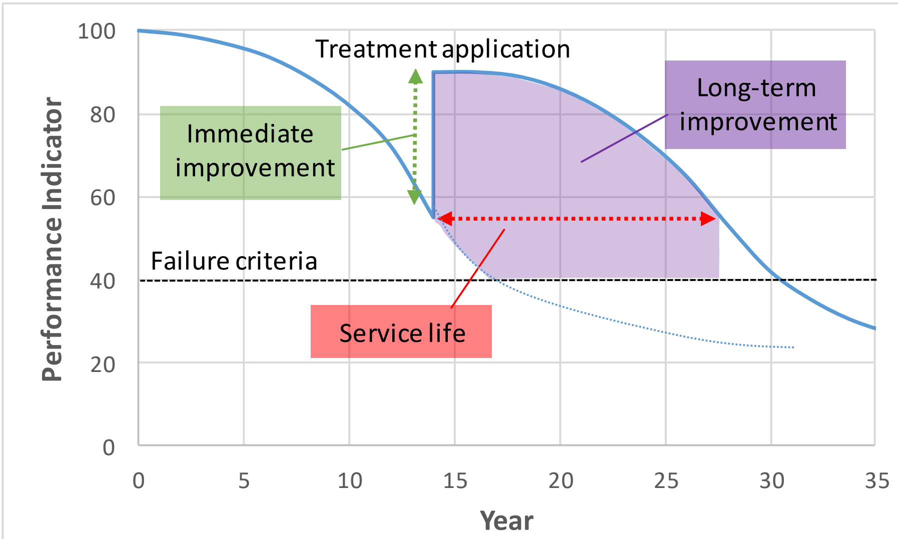

Figure 4: Schematic diagram of Life cycle cost analysis of a pavement

2.4 Pavement Treatments to Reduce Crashes by Increasing Friction

This section defines each treatment and summarizes performance data as shown in Table 4 :

- High friction surface treatment (HFST)
- Seal coat (chip seal)
- Thin asphalt overlay
- Permeable friction course
- Water blasting (for flushed seal coats)

One recent and thorough research report on these treatments was performed by (Merritt, Lyon, & Persaud, 2015), sponsored by the Federal Highway Administration.

2.4.1 High Friction Surface Treatment

HFST is a safety-first pavement treatment intended to restore and maintain pavement friction to reduce crashes, especially around horizontal curves during wet weather (Julian & Moler, 2008). It is a thin layer of high-quality polish-resistant aggregate bonded to the pavement surface with polymer resin binder (see Figure 5). The most common aggregate used is calcined bauxite and the binder is often an epoxy resin or polyester resin.

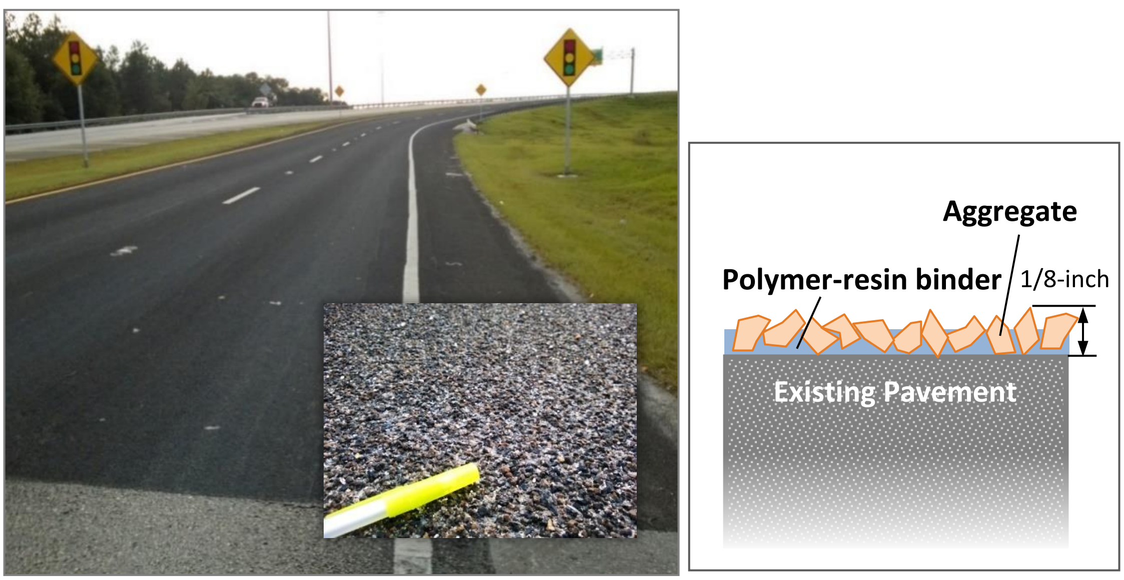

Figure 5: High Friction Surface Treatment

2.4.2 Seal Coat

Seal coats, also known as chip seals and surface treatments, are a common inexpensive maintenance surface treatment in which a layer of asphalt emulsion or other asphalt binder spray applied and overlaid by aggregate to seal the surface against oxidation and moisture (see Figure 6). Seal coats also provide a new aggregate wearing surface which improves skid resistance (Douglas D Gransberg & James, 2005). Loss of skid resistance will occur over time, not just with polishing, but as the aggregates are shifted into more flat positions and especially as bleeding occurs (asphalt migrating to the surface.)

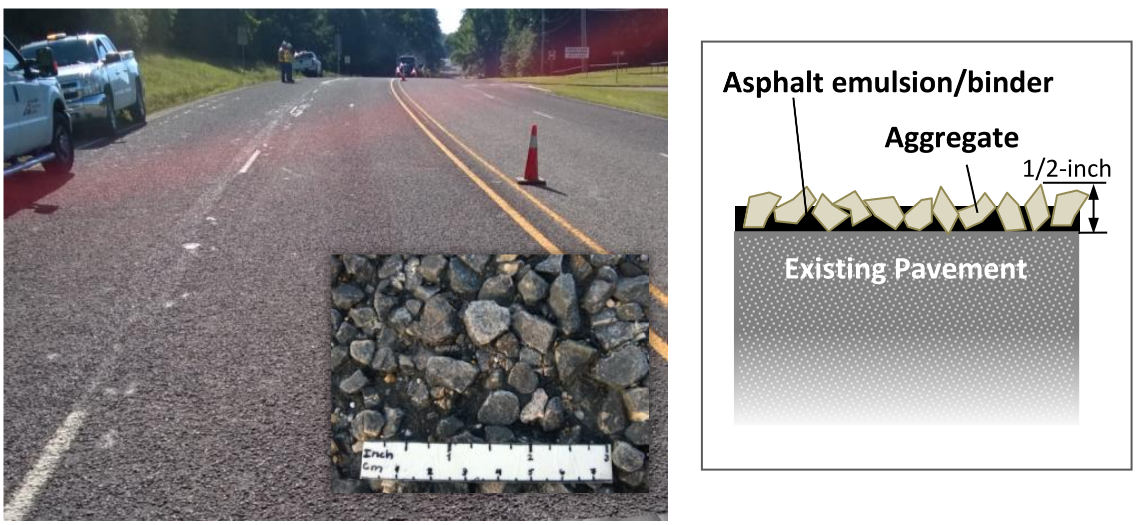

Figure 6: Seal Coat

2.4.3 Thin Asphalt Overlay

A thin asphalt overlay is a thin lift of dense- or gap-graded asphalt concrete, less than 1.5 inches thick (see Figure 7). They are used primarily for maintenance purposes and provide little in the way of structural capacity. Thin overlays are more expensive than seal coats but have the added benefit of resisting severe traffic movements (start-stop and turning), improving ride quality, and reducing noise. For these reasons, they are more often used for urban areas.

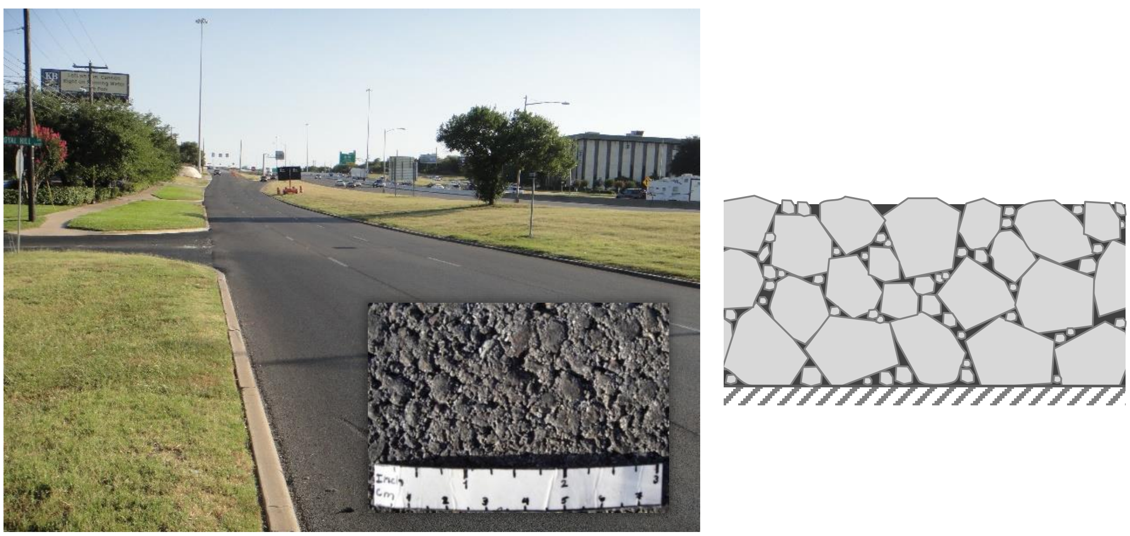

Figure 7: Thin Asphalt Overlay

2.4.4 Permeable Friction Course

A permeable friction course (PFC), (or open graded friction course (OGFC)) is an open-graded hot mix asphalt concrete laid at 1 to 2 inches thick (see Figure 8). It provides functional improvement to the existing pavement in terms water removal, reduced splash and spray, and skid. It is used in the areas of heavy rainfall but often not in colder climates due to inefficiency in freeze-thaw cycles and problems with black ice. PFC often uses higher quality materials than typical dense-graded hot-mix asphalt (HMA) since the durability is compromised by the open-graded design.

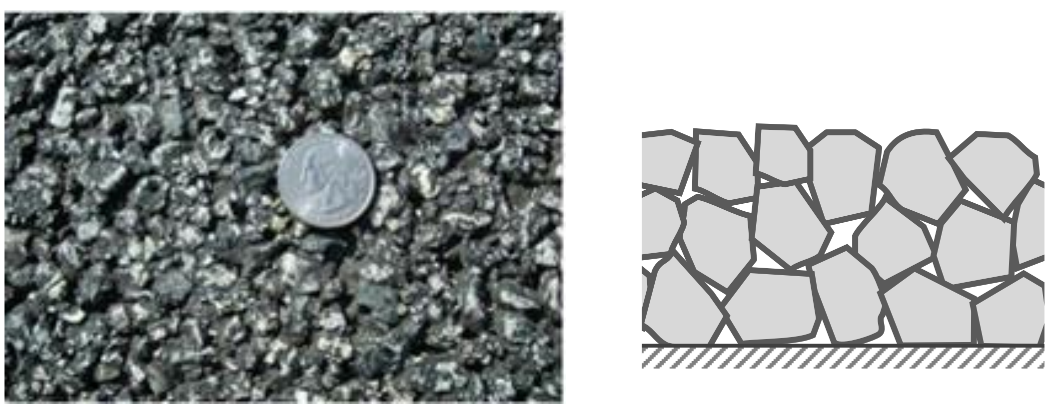

Figure 8: Permeable friction course

2.4.5 Friction Abrading and Pavement Texturing

Diamond grinding is the process of remove a thin layer of Portland cement concrete (typically less than 0.25 inch) with closely spaced saw blades. The process removes surface irregularities and improves skid resistance. Diamond grooving is a treatment in which the pavement surface is saw-cut (usually longitudinally) forming narrow grooves about 0.75 inches apart (see Figure 9).

Figure 9: Grooved Surface (left) and Diamond Grounding (right)

Micro-milling, unlike diamond grinding, uses impact technique in which milling teeth would shave the surface to improve surface friction. Shot blasting or abrading removes the very top-most surface of concrete by projecting thousands of steel pellets or "shots" against the pavement, wearing off the aged surface. The loose shot is continuously picked off the pavement in the process.

2.4.6 Water Blasting

Water blasting is an emerging technology that uses ultra-high pressure water to remove excess binder and impurities from a flushed seal coat pavement surface. The macrotexture of the road is restored, thus improving skid resistance (see Figure 10). The process does not improve the surface texture of the aggregate. Fine jets of ultra-high pressure water (36,000 psi) are directed onto the road surface at an ultrasonic velocity (Mach 1.5) (Lawson, 2006).

Figure 10: Effects of Water Blasting Test

2.5 Treatment Performance and Cost

2.5.1 Service Life of Pavement Treatments

Service life is partially dependent on the existing pavement condition, traffic severity, and climate severity. Table 5 gives the typical service lives of pavement treatments obtained from a survey with contractors. A longer service life, particularly with high skid performance, increases the long-term benefit of a given safety treatment.

Table 5: Service Life for Various Pavement Treatments from a Survey

Treatment Type	Approximate Service Life, yr	Source
HFST	7-12	(Cheung, Julian, & Moravec, 2014)
Seal Coats	3-15	(Morian, 2011)
Thin Asphalt Overlays	8-15	(Wu, Groeger, Simpon, & Hicks, 2010)
Permeable Friction Course	10-15	(Wade, R.l DeSombre, & Peshkin, 2001)
Water Blasting	Data not available	(Lawson, 2006)

2.5.2 Approximate Costs of Pavement Treatments

Table 6 shows approximate unit costs of different treatment types. The most expensive treatment is HFST and the cheapest are seal coats and water blasting. Some of these costs would change depending on the treatment thickness.

Table 6: Unit Cost for Various Pavement Treatments

Treatment Type	**Approximate Unit Cost**	**Source**
HFST	$21/yd²$	(Cheung et al., 2014)
Seal Coats	$1-$2.50/yd²$	(Morian, 2011)
Thin Asphalt Overlays	$3-$6/yd²$	(Wu et al., 2010)
Permeable Friction Course	$7/yd²$	(Wade et al., 2001)
Water Blasting	$1/yd²$	(Lawson, 2006)

2.6 Pavement Friction Mechanisms

2.6.1 Skid Resistance and Pavement Texture

Skid resistance is a property of the surface friction characteristics and contributes to tire-pavement interaction (Noyce, Bahia, Yambó, & Kim, 2005). It is a force contributing to driver’s safety to provide sufficient friction on roads, especially on horizontal curves with wet-weather characteristics such that vehicle can accelerate, maneuver and stop safely (Dewey, 2001; Li, 2005).

During tire-pavement interaction, rubber of the tire undergoes two mechanisms: hysteresis and adhesion (see Figure 11). Hysteresis is a mechanism in which friction generates from the loss of energy due to deformation of the tire rubber along protrusions and depressions of the pavement surface (Linder, Kröger, Popp, & Blum, 2004). The energy loss occurs in the form of heat and noise due to the alternate compression and expansion of the rubber along the macrotexture or asperities of the pavement (Choubane, Holzschuher, & S.Gokhale, 2004). Looking at a bigger picture, hysteresis occurs very frequently when a vehicle is in high speed causing gradual net loss of energy or hysteresis (Linder et al., 2004). Adhesion, on the other hand is a molecular level mechanism that contributes to adherence or an attractive force between tire rubber and the surface of an aggregate (Dewey, 2001). Yandell investigated texture scales relation to hysteresis mechanism (Yandell, 1971). A report showed that tire sliding at high speed contributes to high hysteresis value while tire sliding at low speed contributes to high adhesion value (Kummer & Meyer, 1963).

Researchers investigated that mix design parameters including gradation, bin percentage, aggregate sources etc. had a significant effect on rubber tire skid resistance and texture (Davis, 2002).

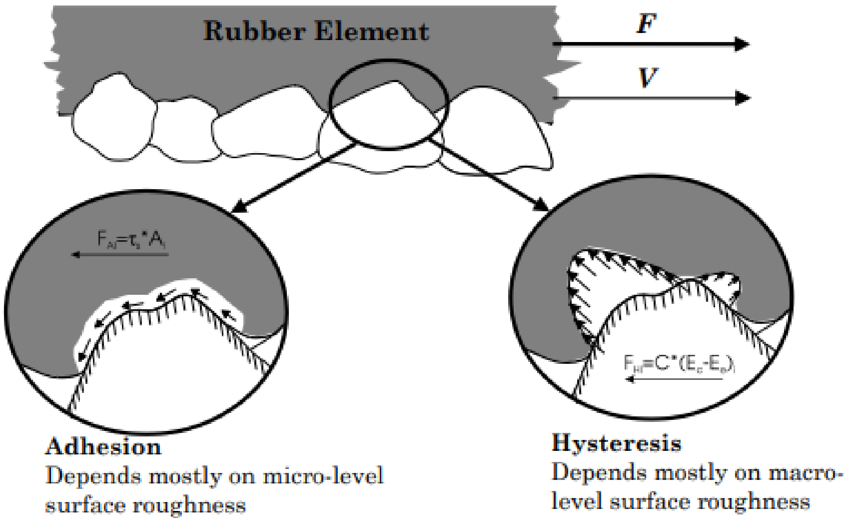

Figure 11: Key Mechanisms of Pavement-Tire Friction (J W Hall et al., 2009)

Reprinted from (J W Hall et al., 2009)

Pavement skid resistance is primarily a function of surface texture characteristics that are technically referred as macrotexture and microtexture (ASTM, 2007; Kummer & Meyer, 1963) as shown in Figure 12. Macrotexture depicts a larger view of asperities on the pavement's aggregate particle matrix while microtexture depicts a smaller view of texture depending on shape, size, angularity, petrology of aggregates, surface of the binder and rubber particles from the tire (Noyce et al., 2005; Roberts, Kandhal, Brown, Lee, & Kennedy, 1996). Macrotexture is defined as a texture on the pavement's aggregate particle matrix or the large asperities that cause hysteresis mechanism. From past research, macrotexture can be a function of aggregate gradation, angularity of coarse aggregates, aggregate type and the type of surface treatment used on the pavement (Noyce et al., 2005). Micro-texture is defined on microscopic scale as it works on the phenomena called adhesion (Noyce et al., 2005; Roberts et al., 1996), in which tire rubber interacts with the texture on the face of aggregates and binder. It contributes to the smoothness or roughness of the aggregate surface and its performance depends on the retention of the roughness against polishing or abrasion by traffic movement and weather (Jayawickrama, Prasanna, & Senadheera, 1996; Noyce et al., 2005). Microtexture provides better traction in dry road surface condition by controlling contact between pavement and tire surface (Arambula et al., 2013).

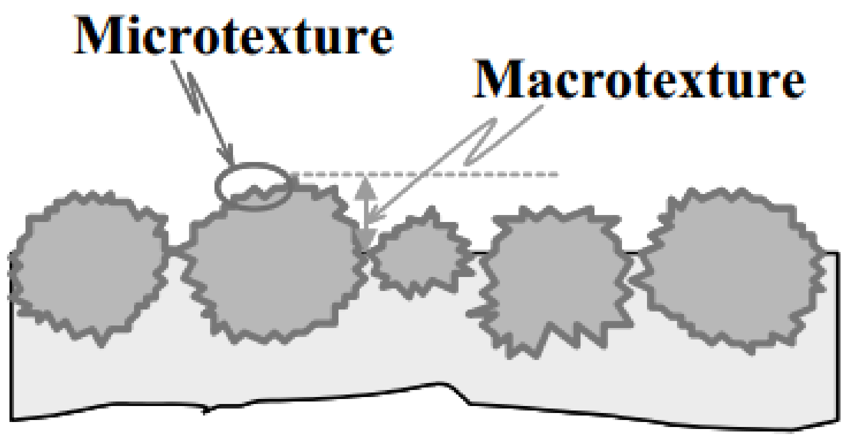

Figure 12: Microtexture & Macrotexture (Flintsch, León, McGhee, & Al-Qadi, 2003)

Reprinted from (Flintsch et al., 2003)

Surface irregularities are categorized into four different ranges of texture: microtexture (wavelength is less than 0.5 mm), macrotexture (wavelength is in the range between 0.5 mm to 50 mm), megatexture (wavelength ranges between 50 mm to 500 mm) and roughness (wavelength greater than 500 mm) (see Figure 13) (Dewey, 2001). Texture wavelengths depict the length between physically repeating features, in this case it is the asperities on the aggregate surface.

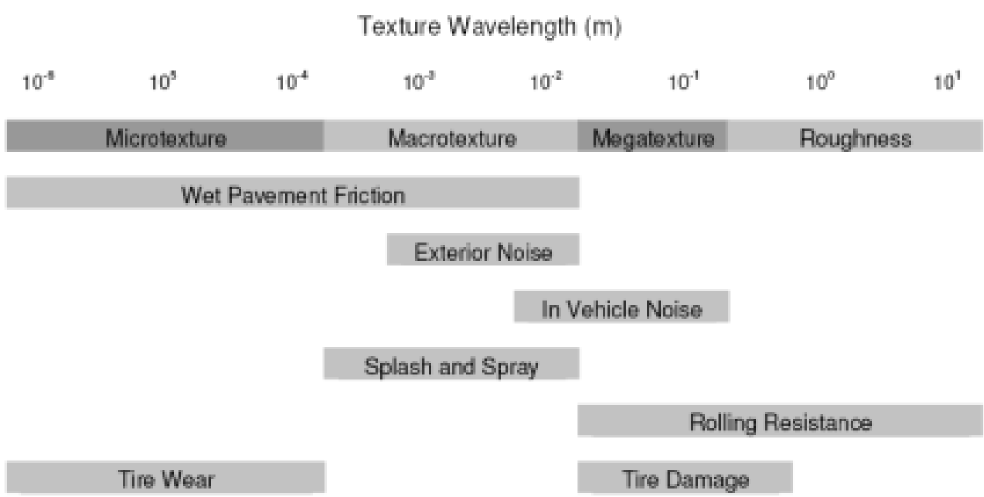

Figure 13: Texture Wavelength Influence on Pavement-Tire Interactions (J. W. Hall et al., 2006)

Reprinted from (J. W. Hall et al., 2006)

Macrotexture allows water to escape out under the tire which prevent hydroplaning. If water stays on the surface of aggregate, it allows slipping of the tire (hydroplaning) and cause run-off crashes or injuries due to sliding. Thus, it contributes to hysteresis mechanism when a tire deforms while moving on asperities and causing energy loss (Dewey, 2001; Ergun, Iyinam, & Iyinam, 2005; Forster, 1989). Bloem investigated that the texture wavelength should be at minimum 0.5 mm to allow water to escape from the tire-pavement contact area (Bloem, 1971). Despite macrotexture contributes in the escape of water, microtexture also plays a significant role in maintaining the direct contact between tire and pavement by penetrating through thin film of water by its micro-asperities (Do, Zahouani, & Vargiolu, 2000). Researchers showed that drainage of water is significantly related with the microtexture (Do et al., 2000; Taneerananon & Yandell, 1981).

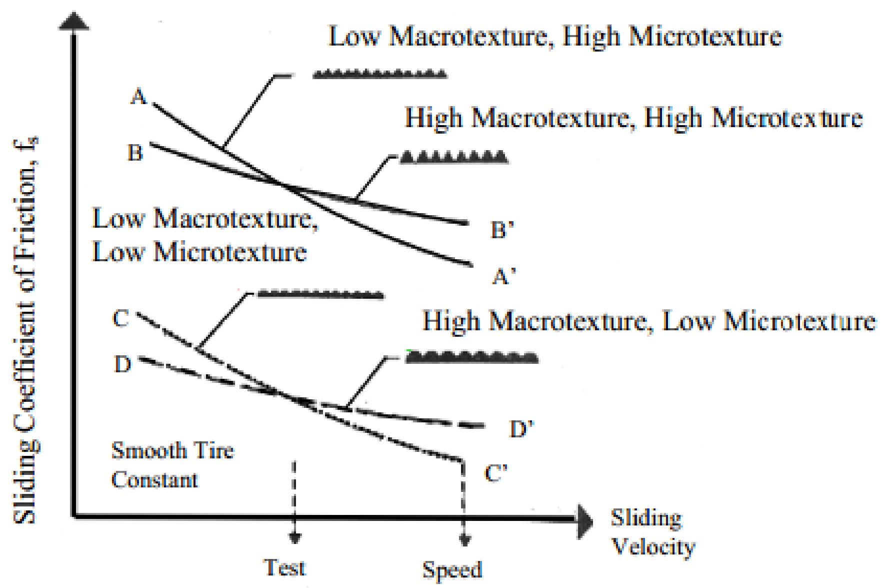

Figure 14: Schematic diagram to show the effect of microtexture/macrotexture on pavement friction (Noyce et al., 2005)

Reprinted from (Noyce et al., 2005)

2.7 Masad-Kassem-Chowdhury Friction Model

Research has developed skid prediction model for hot mix asphalt (HMA) and seal coat surface treatments. The model considered aggregate shape characteristics (angularity and texture indices) from laboratory measurements, gradations and friction measurements from lab and field tests. A mathematical model was developed for gradation of aggregates and a statistical model was developed for friction. Figure 15 shows the flowchart explaining the inputs and outputs of the model.

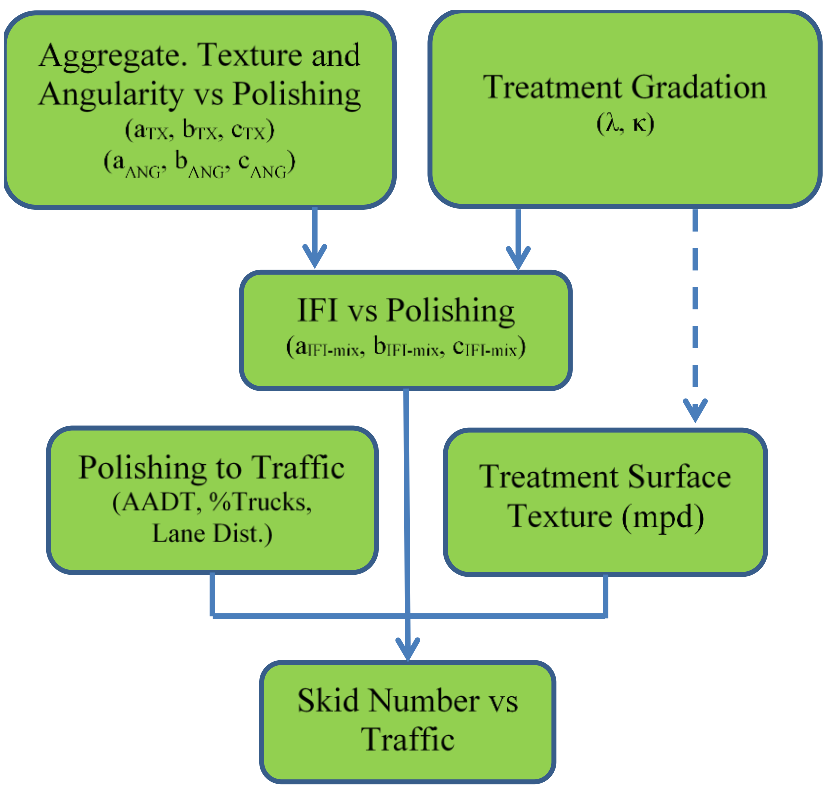

Figure 15: Flowchart explaining modelling approach

The researchers measured aggregate shape characteristics (angularity and texture indices) using the Aggregate Measuring System (AIMS) at three different polishing or abrasion levels: before micro deval (0 minutes), after micro-deval at 105 minutes (AMD105) and after micro-deval at 180 minutes (AMD180). The researchers developed an aggregate characteristic model to predict angularity and texture indices at AMD180 (Masad, Chowdhury, Kassem, & Aldagari, 2017).

$$TX\ (t) = \ a_{TX} + b_{TX} * e^{(-C_{TX} * t)} \tag{4}$$

$$GA\ (t) = \ a_{GA} + b_{GA} * e^{(-C_{GA} * t)} \tag{5}$$

where,

TX (t) = change in texture (time function) in minutes

a_{TX}, b_{TX}, C_{TX} = regression constants for aggregate texture

t = time taken to polish aggregates in Micro-Deval

GA (t) = change in angularity (time function) in minutes

a_{GA}, b_{GA}, C_{GA} = regression constants for aggregate angularity

Gradation parameters were analyzed using Weibull distribution to fit the aggregate size distribution by shape and scale parameters.

$$F(x, \lambda, \kappa) = 1 - e^{-\left(\frac{x}{\lambda}\right)^{\kappa}} \tag{6}$$

where,

x = aggregate size (mm)

κ, λ = shape and scale parameters respectively

Researchers modified an existing IFI equation in ASTM E274 (equation 7) to evaluate the calculated and measured skid numbers in the study (Masad et al., 2017).

$$IFI = 0.045 + 0.925 \times 0.01 \times SN(50)e^{\frac{20}{S_p}} \tag{7}$$

where,

SN (50) = skid number measured at 50 mph using smooth tire

IFI= international friction index

S_p = speed constant parameter

Modified IFI equation is as shown:

$$SN\ (50) = 4.81 + 140.32(IFI - 0.045)e^{\frac{-20}{S_p}} \tag{8}$$

The predicted SN(50) from equation 8 were compared to find the correlation between measured SN(50) in the field by preforming skid trailer test at 50 mph.

$$IFI\ (N) = a_{mix} + b_{mix} \times e^{(-C_{mix} * N)} \tag{9}$$

$$S_p = 14.2 + 89.7MPD \tag{10}$$

$$MPD = \left(\frac{\lambda}{34.180}\right) - \left(\frac{0.398}{\kappa}\right) + (k^{0.416}) - 0.003N \tag{11}$$

$$N = TMF \times 10^{\frac{1}{A + B \times C_{mix} + \frac{C}{C_{mix}}}} \quad (12)$$

$$TMF = \frac{Days\ between\ construction\ and field\ testing \times adjusted\ traffic}{1000} \quad (13)$$

$$Adjusted\ traffic = \frac{AADT \times (100 - PTT) \times DL_{AADT}}{100} + \frac{AADT \times PTT \times DL_{truck} \times 20}{100} \quad (14)$$

where,

$a_{mix} + b_{mix}$ = initial IFI

a_{mix} = terminal IFI

C_{mix} = rate of change in IFI

TMF = traffic multiplication factor

AADT = average annual daily traffic for a section

DL_{AADT} = design lane factor of AADT (function of no. of lanes & urban/rural condition)

DL_{truck} = design lane factor of trucks (function of no. of lanes & urban/rural condition)

PTT = percent truck traffic

Equation 4 and Equation 5 (Kassem, Awed, Masad, & Little, 2013; Mahmoud & Masad, 2007; Masad et al., 2017) were established to depict the texture and angularity loss with polishing (Micro-Deval test for 0, 105 and 180 minutes). TxDOT recommends polishing aggregate for 0 and 105 minutes but researchers investigated on 180 minutes as well to analyze the effects of polishing for a longer period.

Table 7 shows numerous studies and their observations based on the parameters which were considered to model skid prediction.

Table 7: Suggestions from past research on skid resistance

Findings	**Sources**
skid resistance decreases with speed	(Henry, 1986)
skid resistance decreases with the increase in the temperature of tire rubber	(Shafii, 2009)
skid resistance decreases with the bleeding of asphalt binders on the surface	(Sullivan, 2005)
skid resistance increases with surface grooving	(Pashindu, Fwa, & Ong, 2010)
skid resistance is a function of traffic, pavement texture and compressive strength of concrete	(Ahammed & Tighe, 2007)
test procedure to characterize friction based on polishing rate and terminal friction value	(Kowalski, 2007)
skid resistance is a function of aggregate characteristics, mixture gradation and traffic	(Kassem et al., 2013; Kassem et al., 2012; Masad et al., 2017; Masad, Rezaei, Chowdhury, & Freeman, 2010)

3. PAVEMENT TREATMENT, SKID RESISTANCE, AND AGGREAGATE DATA COLLECTION

3.1 Overview

This section discusses past research, pavement management information system (PMIS), field tests and laboratory tests. Most of the data used on this project was collected from previous projects, additional data was added from field and laboratory tests performed in this project. Test sites were selected based on sharper curve radii and various treatment type. Data for skid resistance and other related parameters were collected. Table 8 shows two categories specifically for Project data and Mix/Treatment data.

Table 8: Types of Data Collected

Project Data	Mix/Treatment Data
- Location - Treatment type - Aggregate type - Construction date - AADT - Curve radius - Skid number etc.	- Gradation - Bin percentages - Aggregate angularity, micro-deval %, texture - Mean profile depth - Coefficient of friction etc.

3.2 Previous Research Data

Table 9 demonstrates the specific source for data extraction; some new data were added to the existing data collected from lab and field tests which will be discussed later in the section.

Table 9: Data Sources from the Literature

Source	Data Description
TxDOT 0-5836 – Performance and cost effectiveness of permeable friction course (Arambula et al., 2013)	PFC - site selection
TxDOT 0-6746 – Validation of asphalt mixture pavement skid prediction model and development of skid prediction model for surface treatments (Masad et al., 2017)	Seal coat- site selection, Aggregate data, Mix data, Friction data
TxDOT 0-6714 – Evaluating the Need for Surface Treatments to Reduce Crash Frequency on Horizontal Curves (M. P. Pratt et al., 2014)	HFST - site selection
TxDOT 0-6615 - Design and construction recommendations for thin overlays in Texas (Wilson, Scullion , & Estakhri, 2013)	Aggregate data, Mix data, Friction data
TxDOT 0-6742 – Evaluation of design and construction issues of thin HMA overlays (Wilson, Scullion, & Faruk, 2015)	Aggregate data, Mix data, Friction data, thin overlay-site selection
FDOT - BDR74-977-05 – Alternative aggregates and materials for high friction surface treatment (Wilson & Mukhopadhyay, 2016)	Aggregate data, Mix data, Friction data, HFST-site selection
TxDOT – 0-5230 – Maintenance solutions for bleeding and flushed pavements surfaced with a seal coat or surface treatment (Senadheera, Henderson, Surles, & Lawson, 2013)	Water blasting-site selection

3.3 Pavement Management Information System (PMIS) Skid Data

TxDOT PMIS (Pavement Management Information System) was accessible which provided historic skid data from 2003 to 2016 maintained by the state. The skid data along with other parameters from the previous research were queried to select new sites for field skid test mentioned in Table 10. A total of 81 projects were queried and selected based on Roadbed ID (type of routes and lanes), beginning and ending Texas Reference Markers (TRM), between first year after paving until the latest known year of its existence.

3.4 Field Skid Data

From central, west and east Texas, 40 sites (see Figure 16 and Table 10) were selected including 8 HMAs (orange), 9 PFCs (blue), 13 seal coats (green), 8 HFSTs (red) and 2 water blasting (yellow) treatments to assess their parameters such as aggregate types, traffic condition, service life etc.

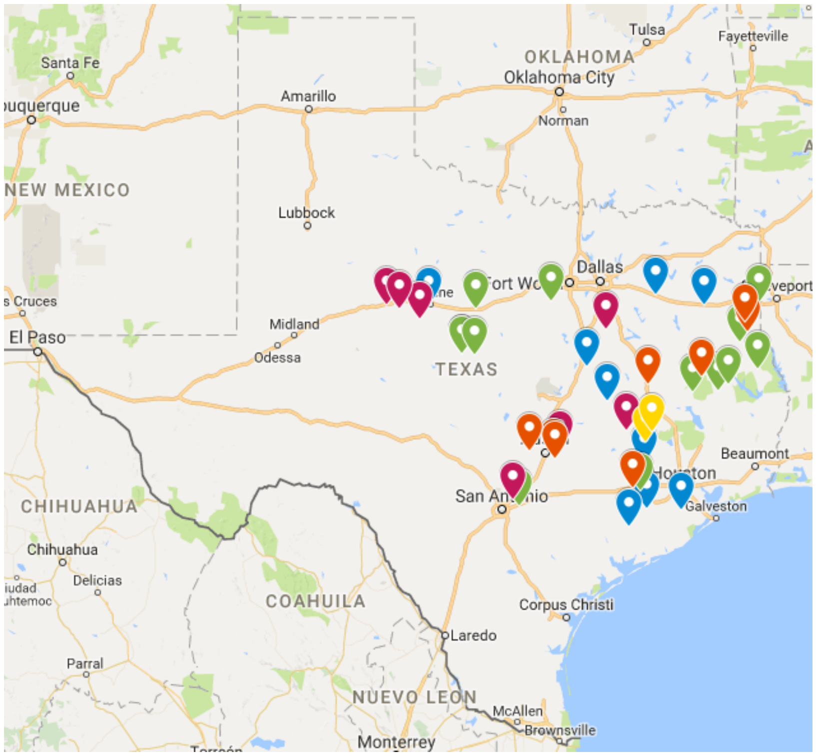

Figure 16: Locations of skid trailer test

Table 10: Selected 40 sites for Field Skid Test

Section Name	Treatment Type	Aggregate Type
HFST-SH 47-Brazos-Bryan	Seal Coat, Bleeding	Calcined Bauxite
HP Water-FM 2562-Grimes-Bryan	Seal Coat, Bleeding	Lightweight (Expanded Shale/Clay)
HMA-IH 45-Leon-Bryan	Seal Coat, Bleeding	Sandstone + Silliceous River Gravel + Limestone
HFST-Kimbro-Travis-Austin	Seal Coat, Bleeding	Calcined Bauxite
HMA-FM 973-Travis-Austin	Seal Coat, Bleeding	Limestone
HMA-SH 71-Travis-Austin	Seal Coat, Bleeding	Sandstone + Limestone
HMA-FM 3238-Travis-Austin	Seal Coat, Bleeding	Sandstone + Limestone
Seal Coat-SH 29-Travis-Austin	Seal Coat, Bleeding	NA
HFST-Lp 1604-Bexar-San Antonio	Seal Coat, Bleeding	Calcined Bauxite
Seal Coat-FM 1518-Bexar-San Antonio	Seal Coat, Bleeding	Sandstone
HMA-IH 10-Austin-Yoakum	Seal Coat, Bleeding	Dolomite-Limestone
Seal Coat-SH 36-Austin-Yoakum	Seal Coat, Bleeding	Limestone
HMA-US 59-Wharton-Yoakum (Hillje)	Seal Coat, Bleeding	Unknown
PFC-US 59-Wharton-Yoakum (Kendelton)	Seal Coat, Bleeding	Limestone
PFC-SH 288-Brazoria-Houston	Seal Coat, Bleeding	Granite + Limestone
PFC-SH 6-Waller-Houston	Seal Coat, Bleeding	Unknown
HP Water-SH 90-Grimes-Bryan	Seal Coat, Bleeding	Lightweight (Expanded Shale/Clay)
Seal Coat-US 287-Trinity-Lufkin	Seal Coat, Bleeding	Lightweight (Expanded Shale/Clay)
Seal Coat-SH 7-Houston-Lufkin	Seal Coat, Bleeding	Lightweight (Expanded Shale/Clay)
Seal Coat-US 59-Angelina-Lufkin	Seal Coat, Bleeding	Traprock
Seal Coat-FM 2213-San Augustine-Lufkin	Seal Coat, Bleeding	Lightweight (Expanded Shale/Clay)
Seal Coat-US 59-Shelby-Lufkin	Seal Coat, Bleeding	Sandstone
Seal Coat-US 59-Panola-Atlanta	Seal Coat, Bleeding	Sandstone
HMA-US 59-Panola-Atlanta	Seal Coat, Bleeding	Quartzite
Seal Coat-US 80-Harrison-Atlanta	Seal Coat, Bleeding	Lightweight (Expanded Shale/Clay)
PFC-IH 20-Smith-Tyler	Seal Coat, Bleeding	Sandstone
PFC-IH 20-Van Zandt-Tyler	Seal Coat, Bleeding	Unknown
HFST-US 287-Navarro-Dallas-A	Seal Coat, Bleeding	Calcined Bauxite
HFST-SH 22-Navarro-Dallas	Seal Coat, Bleeding	Calcined Bauxite
PFC-SH 6-McLennan-Waco	Seal Coat, Bleeding	Limestone
PFC-SH 6-Robertson-Bryan	Seal Coat, Bleeding	Sandstone + Limestone
Seal Coat-US 377-Brown-Brownwood	Seal Coat, Bleeding	Limestone
Seal Coat-US 67-Brown-Brownwood	Seal Coat, Bleeding	Limestone
Seal Coat-US 67-Coleman-Brownwood	Seal Coat, Bleeding	Limestone
HFST-FM 89-Taylor-Abilene	Seal Coat, Bleeding	Calcined Bauxite
HFST-FM 2035-Nolan-Abilene	Seal Coat, Bleeding	Calcined Bauxite
HFST-IH 20-Nolan-Abilene	Seal Coat, Bleeding	Calcined Bauxite
PFC-US 83-Taylor-Abilene	Seal Coat, Bleeding	Limestone
Seal Coat-US 183-Eastland-Brownwood	Seal Coat, Bleeding	Limestone
HMA-US 377-Hood-Dallas-FW	Seal Coat, Bleeding	NA

3.4.1 Locked-Wheel Skid Trailer Test

Locked wheel skid trailer test measures skid resistance in the form of skid number (SN-dimensionless quantity) which is towed at a specific speed along the pavement with either a standard smooth or ribbed tire (see Figure 17). These measurements are taken using a standard tire (SN50S) with a controlled slip condition (0 to 100 percent slip) following guidelines of ASTM E274, E303, E503, E556, E670, E707 (ASTM, 2007; Johnsen, 1997).

Slip condition is further categorized into four main types: locked wheel (force is determined on a 100 percent slip condition), sideway slip (force is determined on a rotating wheel at yaw angle 20^0, fixed slip (wheels at constant slip) and variable slip (user defined slip condition) (Kokot, 2005; PIARC, 1995; Roe, Parry, & Viner, 1998). Locked wheel condition was used in this project with water sprayed simultaneously during the test to simulate the wet pavement condition. Measured torque and vertical load/force applied on a test wheel measure coefficient of friction between tire-pavement interaction. Further, the measured coefficient of friction is multiplied with 100 to determine skid number (SN).

Researchers (Saito, Horiguchi, Kasahara, Abe, & Henry, 1996) mentioned some of the demerits for locked-wheel testers:

- Test is performed at a specific speed and measurements at varying speed can only be measured by repetitive tests at the same section.
- High initial cost and high operation cost (Kummer & Meyer, 1963)

Figure 17: Locked-Wheel Skid Trailer Test

ASTM E274 (Standard Test Method for Skid Resistance of Paved Surfaces Using a Full-Scale Tire) procedure was followed for skid testing, with a skid trailer of smooth tire at a speed of 50 mph. Measured data was further corrected using equation 15:

$$SN_2 = SN_1 + (0.85 * MPD - 1.64) * (V_2 - V_1) \tag{15}$$

where,

SN_2 = Corrected skid number

SN_1 = Measured skid number

MPD = Mean profile depth (mm)

V_2 = Velocity at desired speed (50 mph)

V_1 = Velocity at measured speed

Table 11: Skid Resistance for Various Pavement Treatments

Treatment Type	Test Method	Approx. Skid Number		Comments
		Initial	Long-Term	
HFST	SN40R	70s and 80s	60s	Calcined bauxite
			50s	Flint
Seal Coats	SN60	60s	50s	varies based on aggregate types, mix gradation
Thin Asphalt Overlays	SN (Smooth)	50s	30s	varies based on aggregate types, mix gradation
Permeable Friction Course	SN40R	35-65	20-55	6-yr term

Data collected from these tests were added to the previous data and PMIS queried data to examine it as a single dataset. The values in Table 11 are average results only. The variation of each value within a treatment is large, considering different aggregate types and seasonal variability. Most of these values also represent the skid resistance along simple tangent sections. The skid number around horizontal curves are often much lower that before or after the curve.

Macrotexture is a key component of skid resistance, especially for vehicles traveling at higher speeds and under wet conditions. Again, the values in the Table 11 are typical values only.

3.5 Laboratory Mixture and Aggregate Data

Laboratory tests including aggregate image measuring system (AIMS), micro-deval test, circular track meter (CTM), dynamic friction tester (DFT) and three-wheel polisher was performed on aggregates and mixtures. Slabs were casted with a dimension 500 mm x 400 mm x 44.5 mm (length x width x height) and seal coat surface treatment was applied with different aggregate types. Slabs were tested by CTM (ASTM E2157) and DFT (ASTM E1911) tests to determine mean profile depth and coefficient of friction respectively before and after polishing with three-wheel polisher at 0k, 1k, 5k, 25k and 80k wheel passes for polishing. Aggregates used on the slab were also tested separately to determine their shape characteristics. Aggregates were tested with AIMS to determine their angularity and texture values before and after polishing with micro-deval test at 0, 105 and 180 minutes.

3.5.1 Dynamic Friction Tester (DFT)

The dynamic friction tester (DFT) is used to measure coefficient of friction between the surface and three rubber pads attached to a circular rotating disc (see Figure 18). The circular disc rotates at a linearly increasing speed from 20 to 100 km/hr. The disc lowers gradually after reaching the desired constant speed and touches the pavement surface measuring coefficient of friction (Henry, 1986; Saito et al., 1996).

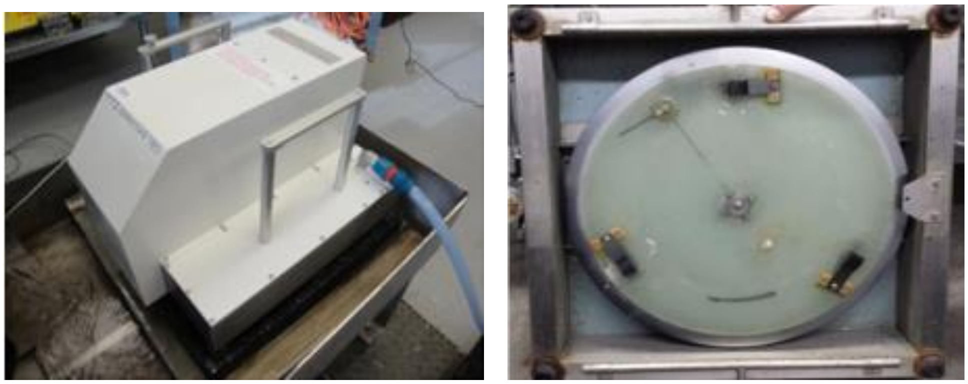

Figure 18: DFT (left) and disc with three rubber pads (right)

3.5.2 Circular Texture Meter (CTM)

CTM is a laser-based device used to measure MPD (mean profile depth) of a pavement and is introduced in 1998 (see Figure 19). It is a portable, user-friendly device which can be used in the field as well as in the lab. A laser sensor is attached to an arm that rotates in a circular profile divided into eight segments/arcs of a circle. A total of 1024 data points is collected in a round and an average Mean Profile depth is calculated according to ASTM E2157 (ASTM-E2157).

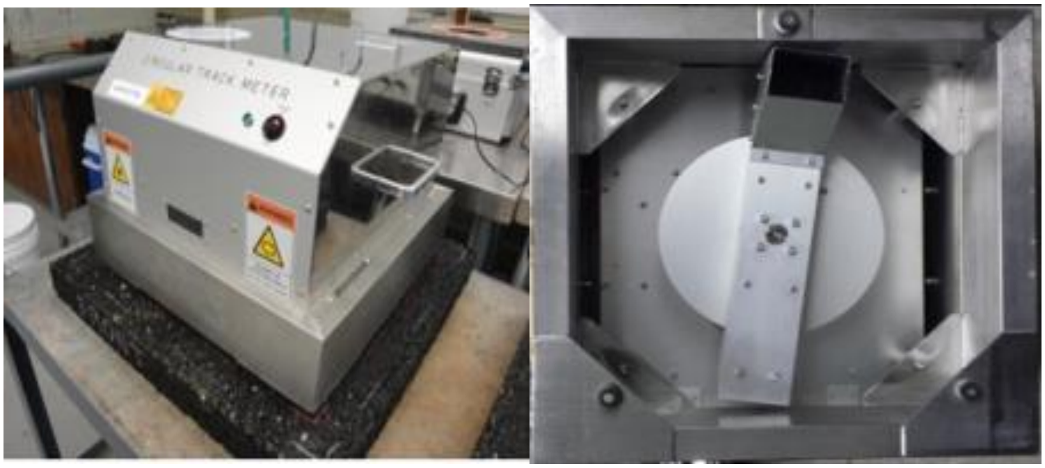

Figure 19: Circular Texture Meter

3.5.3 Three Wheel Polisher

It is a device used to polish the slabs and simulate field traffic condition. It consists of three wheels attached with a turn table and rotate in a circular path at varying cycles as shown in Figure 20. The load applied on wheels can vary by adding or removing circular iron plates on turn table. A laser sensor is attached in the side to detect the number of rotations and is controlled by a digital counter. A water spray assembly consists of three pipes installed to spray water for removing dust/eroded material from the surface.

Figure 20: Modified three-wheel polisher with water bath

Figure 21: Tested sample (after polishing, CTM, DFT)

Table 12: Mean Texture Depth for Various Pavement Treatments

Treatment Type	Approximate Mean Texture Depth, mm
HFST	1.5 to 3
Seal Coats	1 to 3
Thin Asphalt Overlays	0.4 to 0.6 (Dense graded), > 1.0 (Stone Matrix Asphalt)
Permeable Friction Course	1.5 to 3
Abrading and Texturing	0.7 to 1.2 (Grinding), 0.9 to 1.4 (Grooving)
Water Blasting	Varies (depends on aggregate)

3.5.4 AIMS (Aggregate Imaging Measurement System)

The AIMS is used to determine aggregate shape characteristics such as angularity, texture and form by advanced image processing(see Figure 22) (Masad et al., 2017). Aggregates are placed on a tray (transparent or opaque) at a certain distance such that the mounted digital camera captures one aggregate at a time. A top-light and back-light system is installed to provide enough light for clear and sharp images. The aggregate polishing resistance is determined by AIMS test before and after abrading in the Micro-Deval test. Researchers suggested that coarser and angular aggregates provide more skid resistance than the flat and elongated particles (Prowell, Zhang, & Brown, 2005) and aggregates that have rough surface provides higher skid resistance than the smooth surface (Kassem et al., 2013).

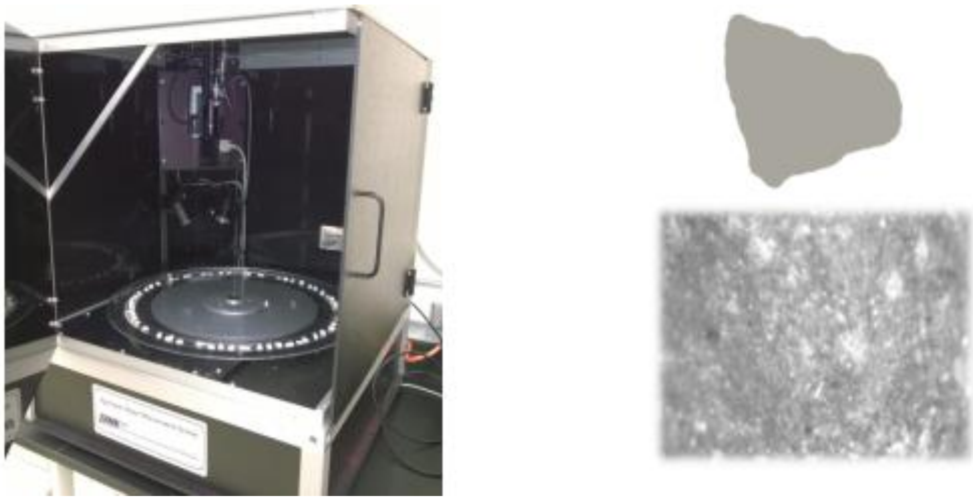

Figure 22: AIMS device (left), Angularity (top-right) & Texture (bottom-right)

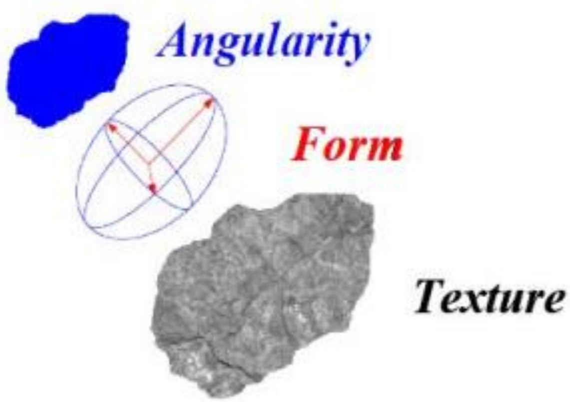

Figure 23: AIMS aggregate shape characteristics (Masad et al., 2017)

Reprinted from (Masad et al., 2017)

3.5.5 Micro-Deval Test

This test is used to estimate the aggregate's ability to resist abrasion or mechanical degradation (J W Hall et al., 2009). It consists of a metallic cylindrical container with approximately 5000 grams of steel balls, the aggregates (test sample-1500 grams) and water (2000 ml) (see Figure 24). The container is then placed on the rollers and is allowed to rotate as per the desired time or rotations following guidelines based on AASHTO T 327-05 test method "Standard Test Method for Resistance of Coarse Aggregate to Degradation by Abrasion in the Micro-Deval Apparatus" and ASTM D 6928 in accordance with Tex-461: Test Procedure for Micro-Deval Abrasion of Aggregate (Kassem et al., 2012).

Figure 24: Micro Deval apparatus (left) and interaction between aggregates and steel balls (right) (Kassem et al., 2012)

Reprinted from (Kassem et al., 2012)

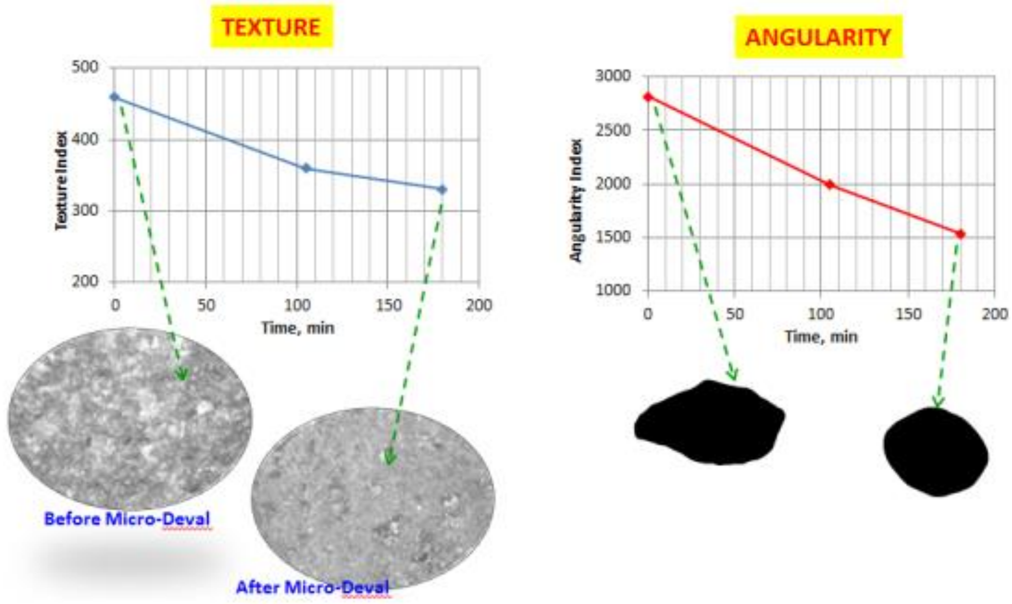

Figure 25: Loss in Aggregate Texture and Angularity as a Result of Micro-Deval Abrasion and Polishing of Virgin Aggregates (Masad et al., 2017)

Reprinted from (Masad et al., 2017)

Researchers suggested that the wet environment established in the micro-deval test simulates better wet-weather related field conditions (Rogers, 1991). Figure 25 shows behavior of an aggregate's shape characteristics with polishing.

4. RESULTS AND DATA ANALYSIS

4.1 Measured Skid Numbers on Field

The results of the field skid testing are shown in Figure 26. The highest skid numbers were measured on HFST sites while the lowest skid numbers were measured on bleeding seal coats. HFST treatment implementation is new to Texas so most of the sites were constructed in the past two years. Generally, HFST treatment provide skid numbers in the 70s because of the aggregate type - calcined bauxite of uniform gradation. Two water blasting sites were still available for testing. One had a high skid number (54) while the other bled again and was considered as bleeding seal coat with a SN value as low as 17. Seal coats had skid numbers with an average of 37 with highs in the 50s to lows in the 20s. HMA and PFC treatments had skid numbers with an average of about 30 with highs in the 40s and lows in the 20s.

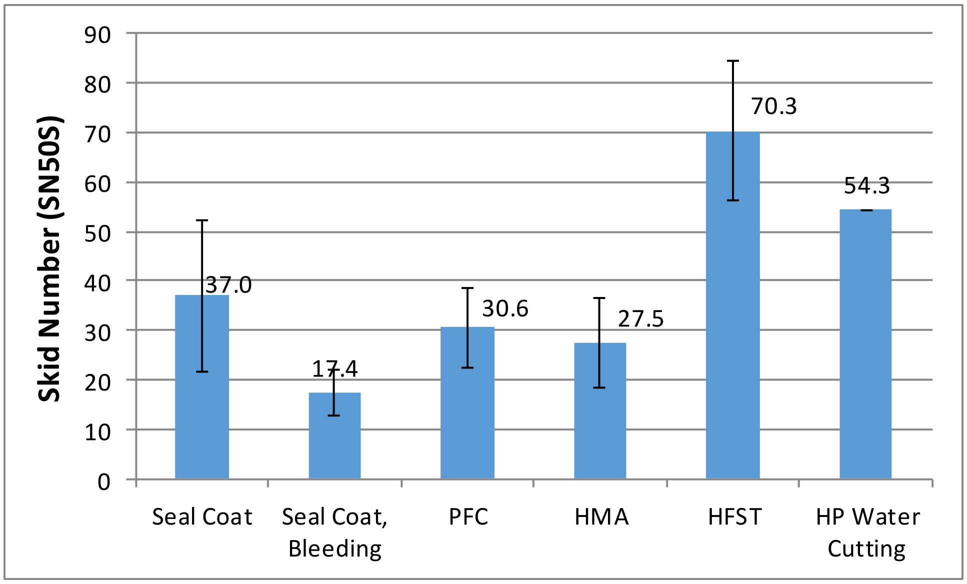

Figure 26: SN values by treatment type measured by Project Team

Figure 27 shows average skid number values based on aggregate type. Calcined Bauxite had the highest skid number value (i.e. 68.2) which supports the previous discussion as this aggregate was only used in HFST installation with highest SN value. Lightweight aggregates i.e. expanded shale and clay had the next highest SN value with an average of 46 ranging between 60s to 30s. SAC A (Surface aggregate classification A) aggregates comprised of quartzite, traprock, sandstone etc. (BRSQC, 2018) ranged between 30 and 50. Limestone and dolomite aggregates had the lowest SN value in 20s.

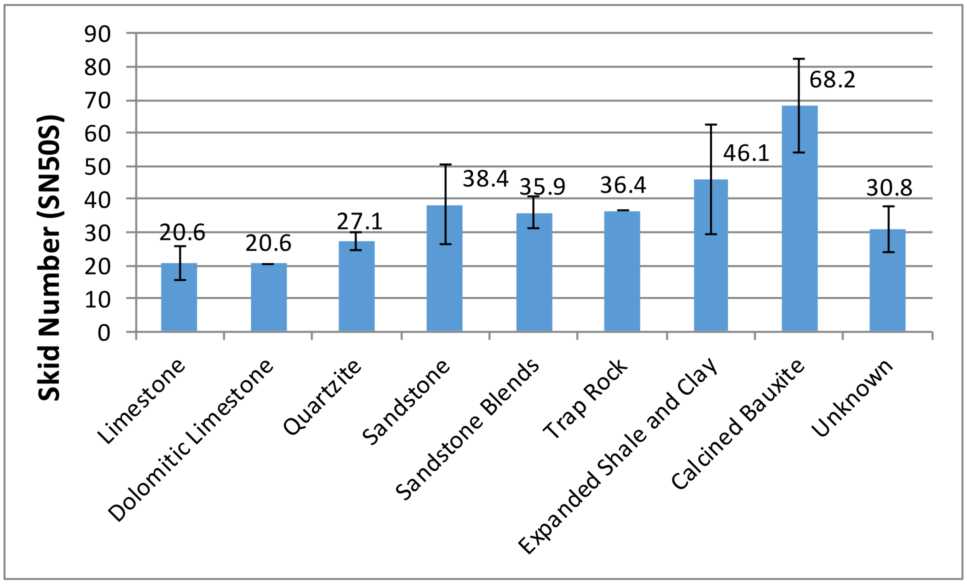

Figure 27: SN values based on Aggregate Type as Measured by the Project Team

Figure 28 showed average skid number based on treatment type. 3318 datasets were collected from TxDOT PMIS, past researches and current study. HFST had the highest average skid number in the 70s while the lowest observed was water blasting treatment. Water blasting treatment is usually applied on flushed seal coat to retrieve its frictional properties. Seal coats had average skid number in the range of 40s while other treatments had a range in between 25 to 40.

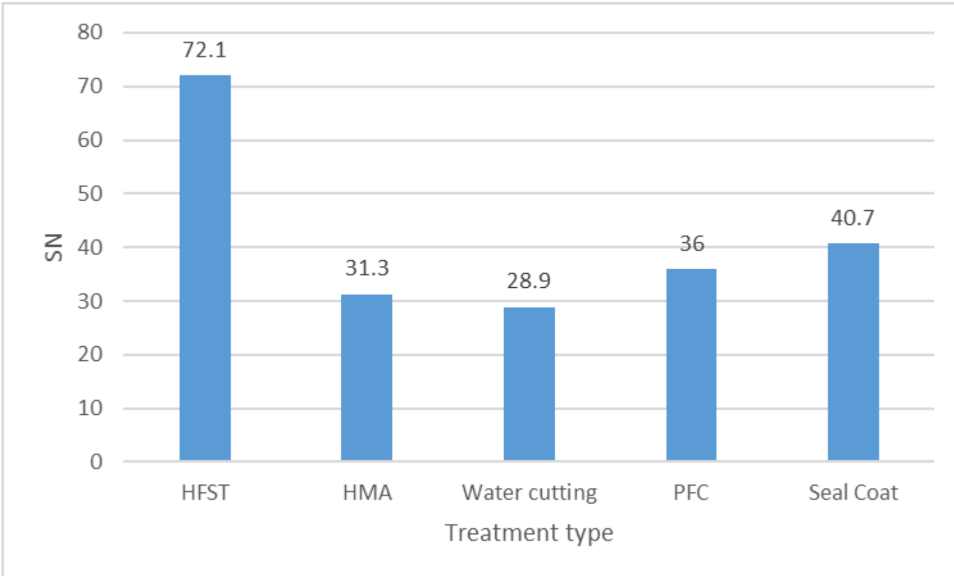

Figure 28: SN based on treatment type as observed by the data collected from PMIS, past researches and current study

4.2 Skid Data Collected from TxDOT PMIS

PMIS data were also queried for SN value based on aggregate type. As mentioned earlier, HFST is new to Texas so calcined bauxite aggregate was not queried from PMIS. Figure 29 manifests that the expanded shale and clay (light weight aggregate) had higher SN value ranging between 50s and 60s. SAC A aggregates had skid numbers between 30s and 40s while limestone and dolomite had the lowest range in 20s.

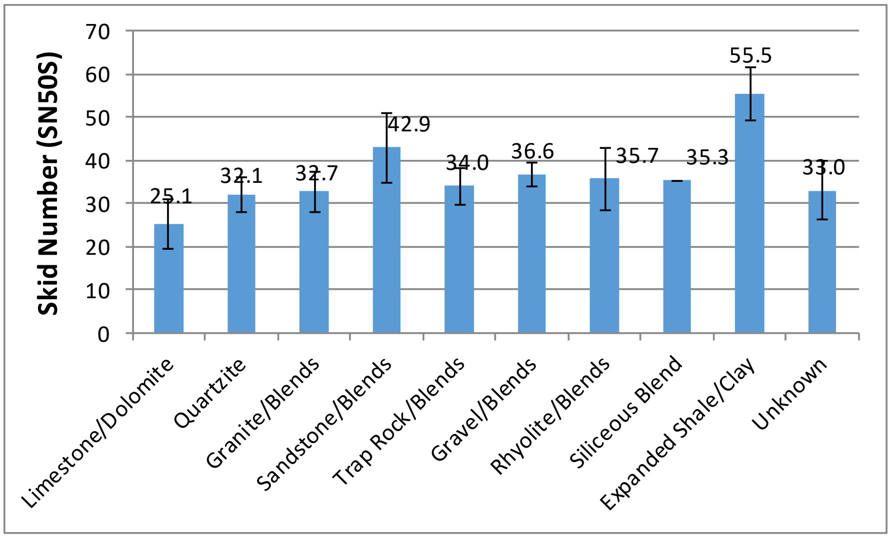

Figure 29: SN value based on aggregate type from PMIS data

From PMIS queried data, skid number for HMA, PFC and seal coat were analyzed and their average values with variation can be seen in Figure 30. Three of the treatments represent the average skid number (in 30s) measured throughout the treatment life; however, seal coat has the maximum variation, ranging from high 50s to low 20s.

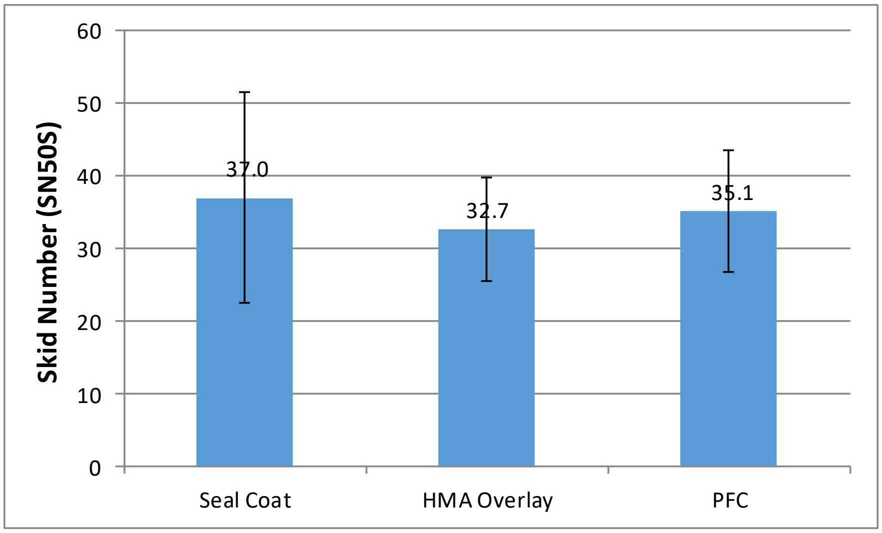

Figure 30: SN value based on treatment type from PMIS data

4.3 Skid data from High Friction Surface Treatment Project

Florida DOT with a combined effort of TTI researchers conducted a research on high friction surface treatment (HFST). HFST had highest skid number around 70s as compared to skid numbers from concrete, open graded and dense graded asphalt treatments ranging between 30s and 50s (Wilson & Mukhopadhyay, 2016)(see Figure 31).

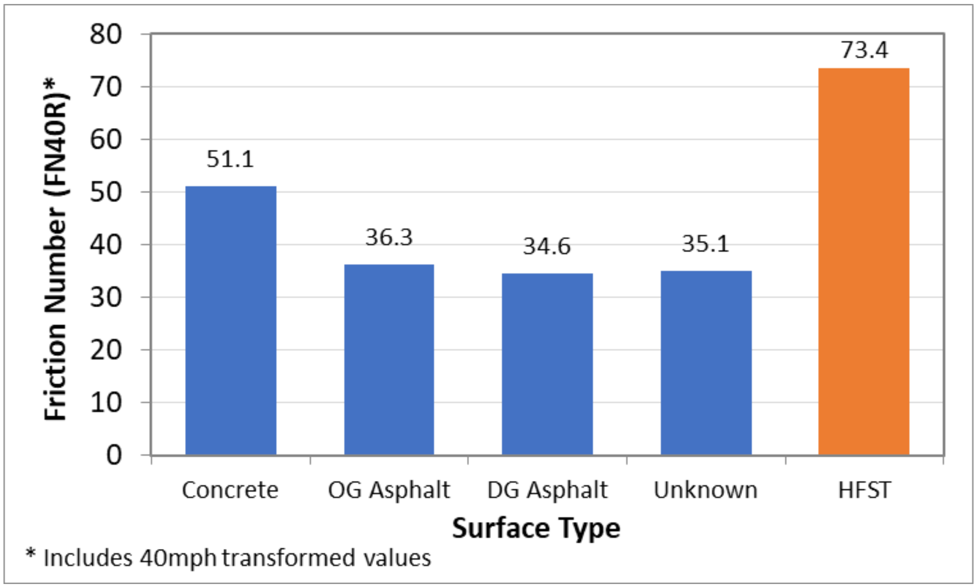

Figure 31: SN values based on treatment type (Wilson & Mukhopadhyay, 2016) Reprinted from (Wilson & Mukhopadhyay, 2016)

4.4 Aggregate Texture, Angularity, and Micro Deval Loss

Aggregate texture, angularity, and micro-deval loss data are shown in Figure 32, Figure 33 and Figure 34. Crushed siliceous and limestone gravel has the lowest angularity reduction (6 percent) as compared to the limestone which has 34 percent reduction. Granite had highest initial angularity while sandstone and limestone had the least. Granite, bauxite and quartzite have texture greater than 300 while limestone and dolomite have the least texture values. Limestone and dolomite has approximately 40-50 percent reduction in texture while bauxite and granite show 5-15 percent reduction. After micro-deval, limestone abrades 24 percent while bauxite abrades only by 5 percent.

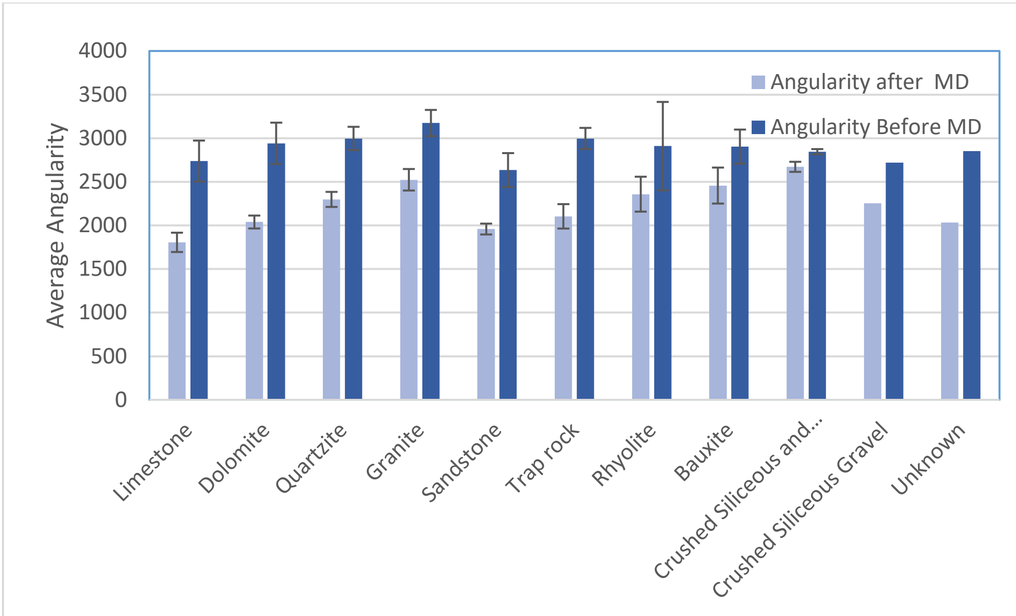

Figure 32: Angularity based on aggregate type from past research (Table 9)

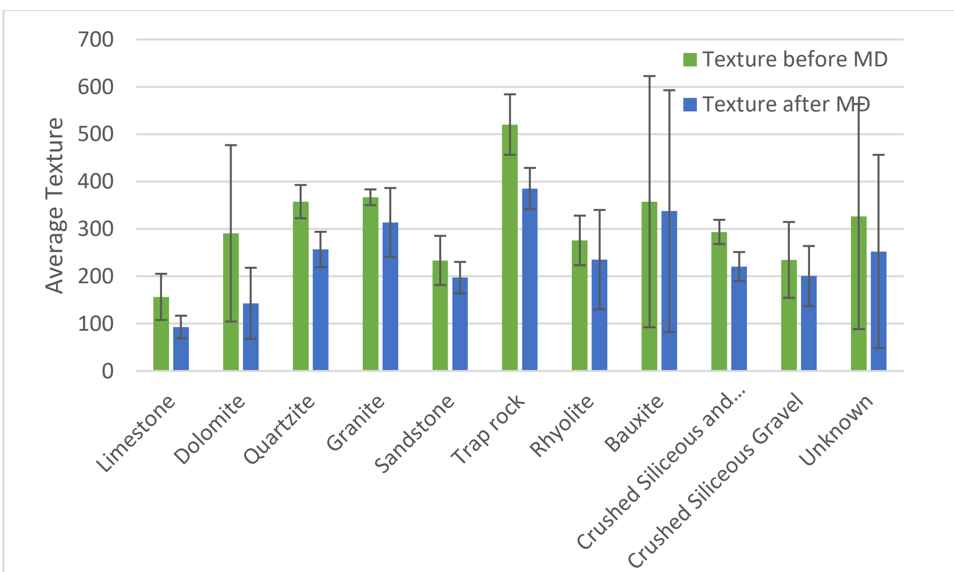

Figure 33: Texture based on aggregate type from past research (Table 9)

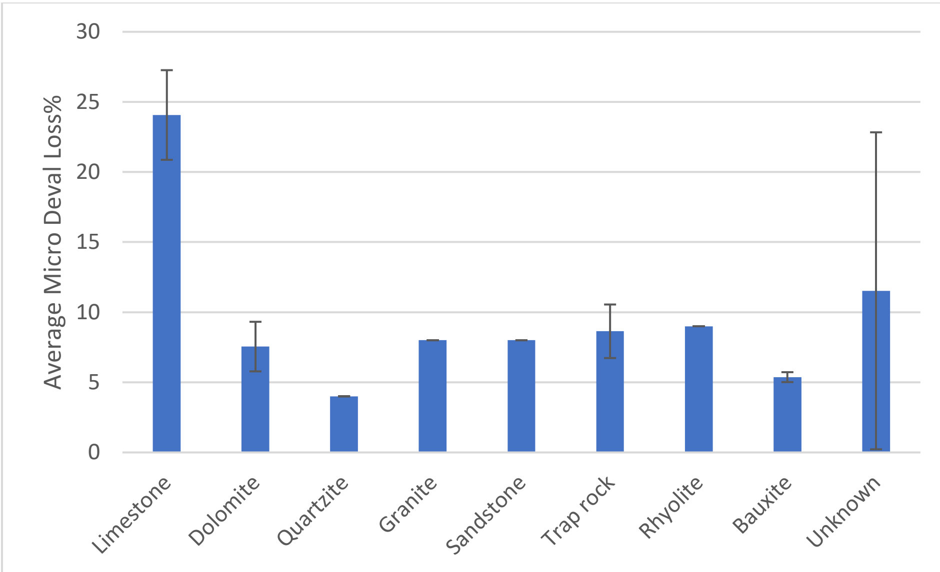

Figure 34: Micro-deval loss % based on aggregate type by past researches (Table 9)

Aggregate testing with the AIMS and micro-deval at 105 minutes is complete for the Streetman and Riverlite lightweight aggregates. It was observed that Streetman Gr 4 showed better performance with minimum percentage loss after polishing in micro-deval (Figure 35).

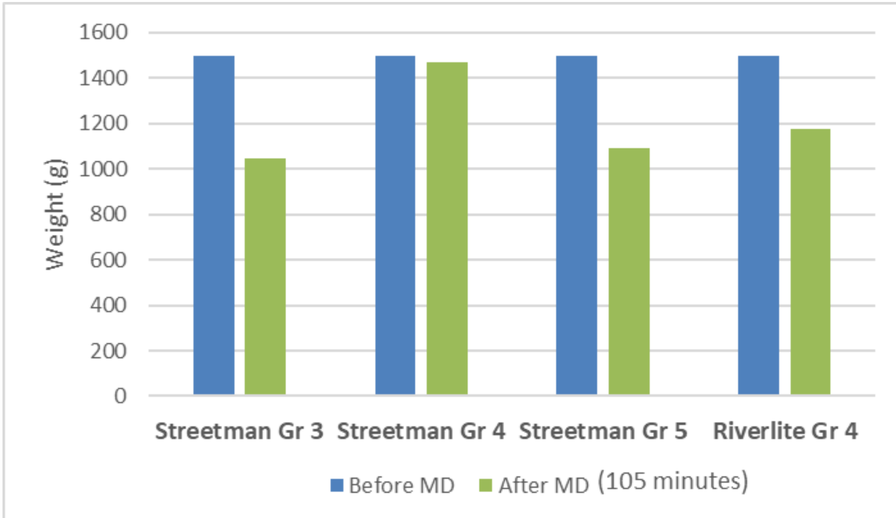

Figure 35: Weight Loss due to Micro-Deval Test as Measured by Project Team

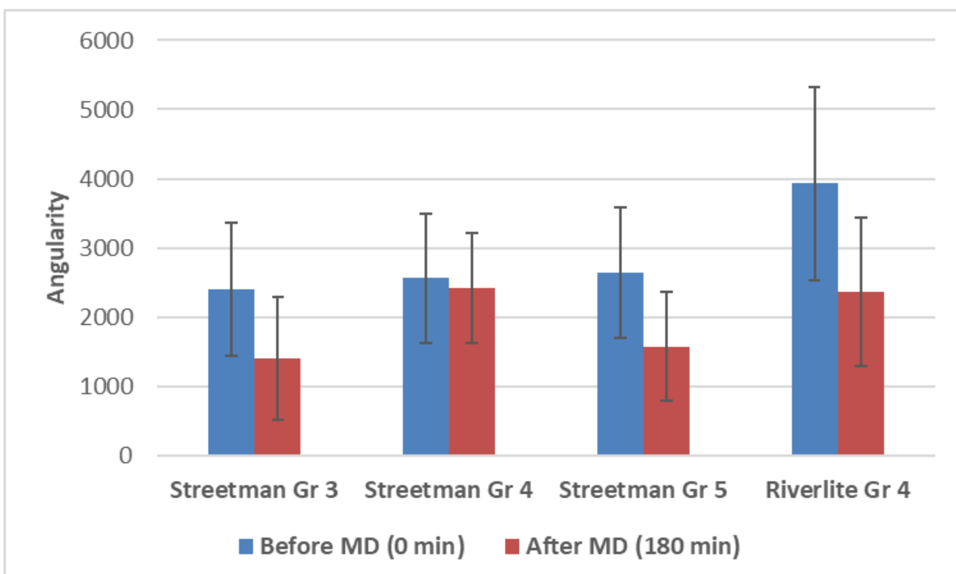

Figure 36: Angularity for Lightweight Aggregates Measured by Project Team

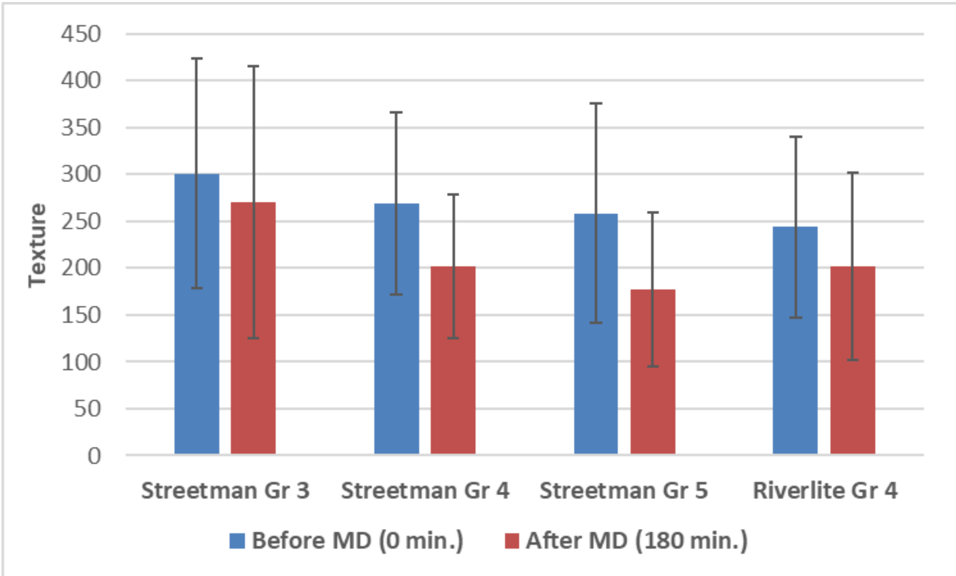

Figure 37: Texture Values for Lightweight Aggregates Measured by Project Team

In Figure 36, Streetman manufactured aggregate had lower initial angularity than the Riverlite aggregate, though both were similar after polishing. Riverlite had slightly lower texture before polishing than Streetman. In Figure 37, initial texture values were approximately in the similar range but Streetman Gr.5 aggregate experienced higher texture loss relatively than the other aggregates.

Figure 38 showed loss in weight of an aggregate before and after polishing (105 and 180 minutes). Crushed gravel from Phar had minimum percent loss than the other aggregates. Light weight aggregates from Streetman and Riverlite sources had a noticeable percent loss like Texas Limestone.

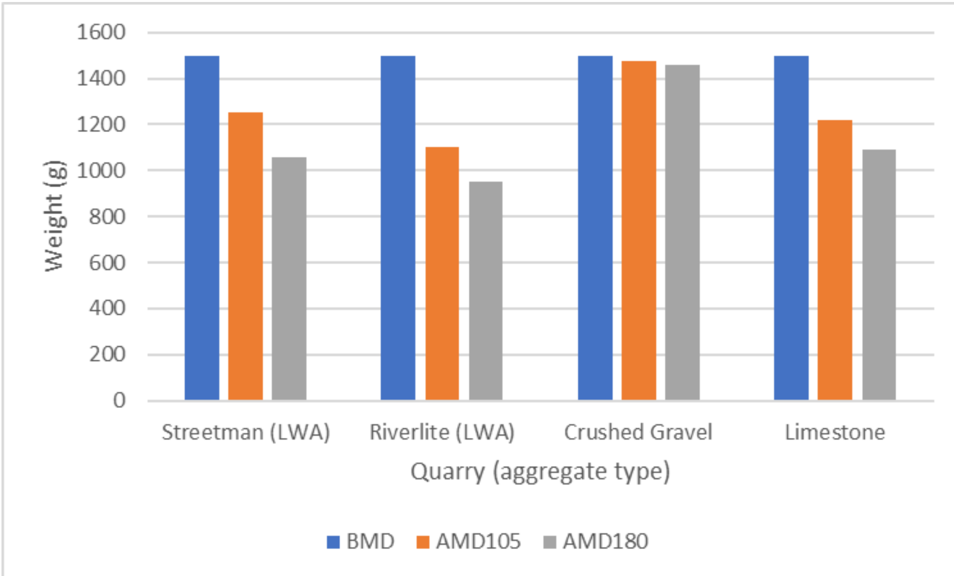

Figure 38: **Weight loss due to micro-deval abrasion**

In Figure 39, light weight aggregates from Riverlite quarry showed higher initial angularity than other aggregates but angularity indices after polishing was in the same range with other aggregates. In Figure 40, limestone had lowest texture value than any other aggregate which was expected as limestone abraded very quickly due to 100% calcite mineral composition

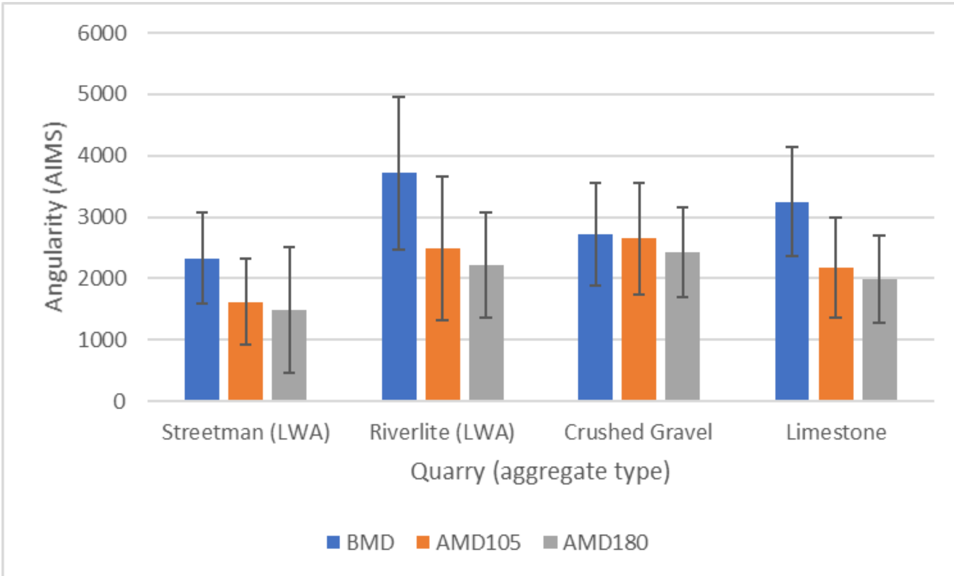

Figure 39: Measured Angularity Values by Project Team

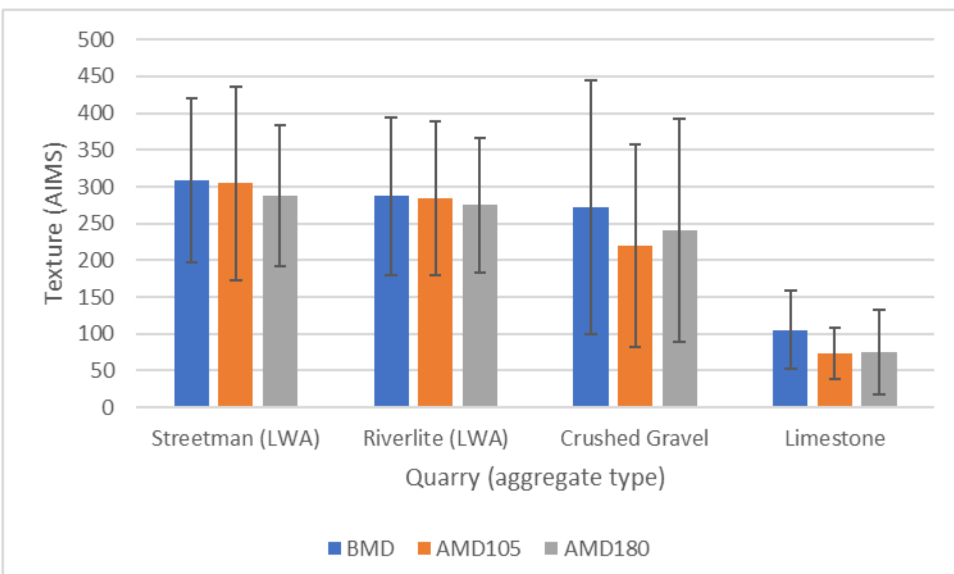

Figure 40: **Measured Texture Values by Project Team**

4.5 Friction and Texture Data on Laboratory Treated Samples

Figure 41 and Figure 42 depicted a sudden drop in texture and friction due to initial cycles of polishing but it went up and then dropped again gradually with the polishing cycles. Aggregates used for seal coat treatment on slabs were bonded with epoxy to hold them well (see Figure 47 to Figure 50).

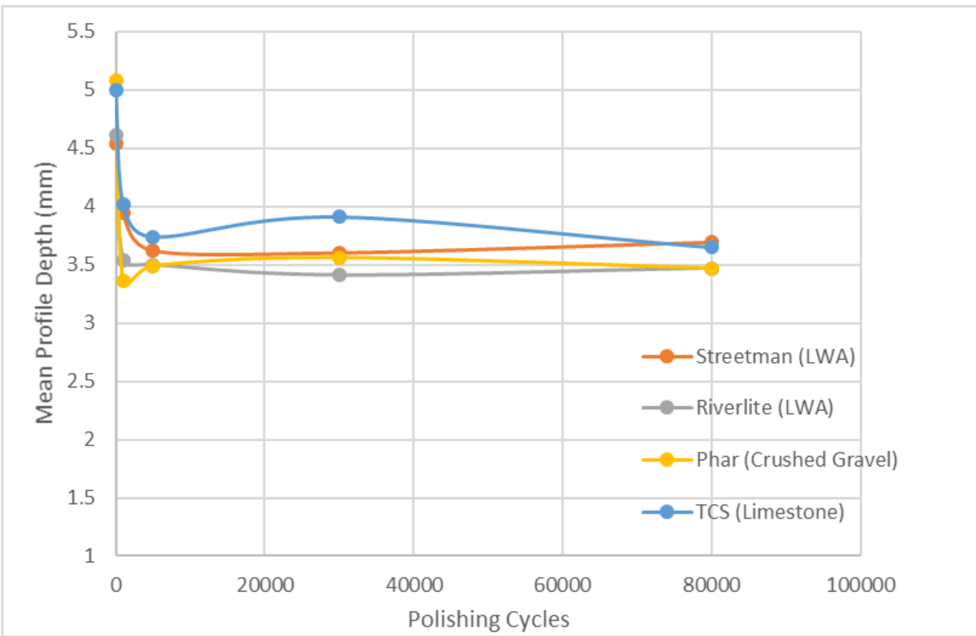

Figure 41: Measured Mean Profile Depth (MPD) by Project Team

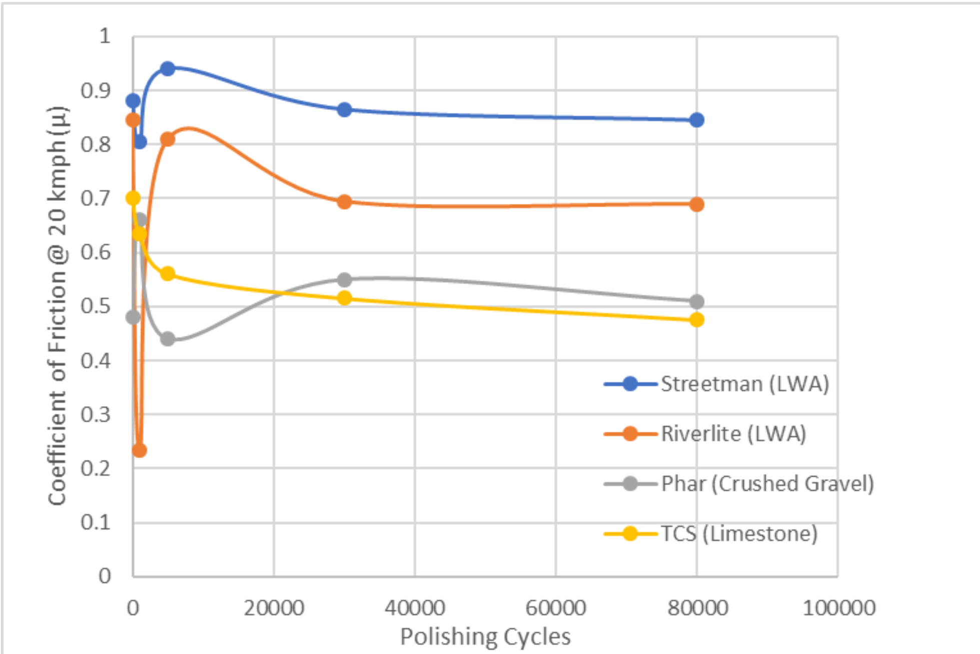

Figure 42: Measured Coefficient of Friction (μ) by Project team

4.6 Proposed Model to Predict Aggregate Shape Characteristics

Data from past research and new data were used to update the Masad-Kassem-Chowdhury model. Aggregate characteristic model was revised including equations and modelling approaches to guard them against overfitting data from small sample sizes which slightly improved the mechanistic representation of the model. Statistical validation to the modelling approach is mentioned in the Figure 43 to Figure 46. Revised aggregate characteristic model focused on predicting shape characteristics (angularity and texture) at 180 minutes polishing. 37 aggregates were tested for angularity and texture indices at 0, 105 and 180 minutes intervals and were utilized to predict angularity and texture values at 180 minutes for the aggregates which did not have angularity and texture values at 180 minutes. These indices of the aggregates vary exponentially with the time (polishing).

$$AMD180_{GA} = -321.20314 + 1.09486^{*} (AMD105_{GA})$$

here,

$AMD180_{GA}$ = angularity index after micro-deval at 180 minutes

$AMD105_{GA}$ = angularity index after micro-deval at 105 minutes

It was found that the angularity index at 180 minutes is highly positively correlated with angularity index at 150 minutes with $R^2 = 0.9798658$ whereas angularity index at 180 minutes is poorly positively correlated with angularity index at 0 minutes with $R^2 = 0.4550294$. The intercept and slope of the angularity index at 105 minutes have p-value of 0.000495 and $2 \times e^{-16}$ respectively at a significance level of 0.05. Diagnostic plots (see Figure 44 and Figure 46) were developed to verify basic assumptions of linear regression viz:

1. Linearity: Relationship between X and the mean of Y is linear.
2. Homoscedasticity: The variance of residual is the same for any value of X.
3. Independence: Observations are independent of each other
4. Normality: For any fixed value of X, Y is normally distributed.

$$AMD180_{TX} = -7.42471 + 0.99791^{*} (AMD105_{TX}) - 0.02117^{*} (BMD_{TX})$$

here,

$AMD180_{TX}$ = texture index after micro-deval at 180 minutes

$AMD105_{TX}$ = texture index after micro-deval at 105 minutes

BMD_{TX} = texture index before micro-deval at 0 minutes

It was found that the texture index at 180 minutes is highly positively correlated with texture index at 150 minutes with R^2 = 0.9967193 whereas texture index at 180 minutes is fairly positively correlated with texture index at 0 minutes with R^2 = 0.8296472. The intercept and slope of texture index@105 minutes had a p-value of 0.0243 and 2e-16 respectively at as significance level of 0.05. Texture Index@0 minutes had a p-value of 0.3388 which showed that the texture Index@180 was not significantly related to texture index@0 minutes. The relationship had an R^2 value of 0.9936. Another model for texture was developed to analyze the effect of texture index at 0 minutes using linear regression,

$$AMD180_{TX} = -8.80147 + 0.97645 * (AMD105_{TX})$$

The intercept and slope of texture index@105 had a p-value of 0.00356 and 2e-16 respectively at as significance level of 0.05. The relationship had an R^2 value of 0.9934.

5. CONCLUSIONS AND RECOMMENDATIONS

5.1 Conclusions

This study was focused on providing information to develop pavement-safety based guidelines and model which eventually would help practitioners to decide a treatment on horizontal curves to reduce crashes. The contributions to the study would help researchers to work with the data collected from past researches, TxDOT PMIS and tests performed by the project team. The following points summarize the primary contributions and conclusions of this study:

- A database was developed including site data (144 sites with various pavement treatments such as HMA, seal coats, HFST, PFC, Water blasting), mix data (contains bin percentage, aggregate source, aggregate type, percent retained on No.4 sieve, gradation), aggregate data (type, source, angularity index, texture index) and skid data (mean profile depth, coefficient of friction).
- An existing model's equations were revised to predict shape characteristics of an aggregate (after micro-deval at 180 minutes) with the help of before micro-deval and after micro-deval at 105 minutes.
- Skid number data was obtained from locked wheel skid trailer test on 40 sites with various treatments such as HMA, PFC, thin overlay, seal coat, seal coat with bleeding and ultra-high-pressure water cutting.

- While most of the treatment including HMA, seal coat, thin overlay had skid number measured on the field in the range between 20 and 50, high friction surface treatment had skid number measured on the field in the range between 55 to 85.
- Based on the statistical analysis, angularity index at 180 minutes was highly positively correlated with angularity index at 150 minutes with $R^2 = 0.9798658$ whereas angularity index at 180 minutes was poorly positively correlated with angularity index at 0 minutes with $R^2 = 0.4550294$.
- Texture Index at 180 minutes was highly positively correlated with texture index at 150 minutes with $R^2 = 0.9967193$ whereas texture index at 180 minutes was fairly positively correlated with texture index at 0 minutes with $R^2 = 0.8296472$.
- CTM and DFT tests were performed on the slabs to add more dataset to the existing data and to compare the mean profile depth and coefficient of friction values for different aggregate types.
- Micro-deval test was performed to determine the percentage loss in weight of different aggregates. Weights were measured before polishing, after polishing at 105 minutes and after polishing at 180 minutes.

5.2 Recommendations

- More aggregates should be tested to increase the dataset and the confidence level of the model
- Mineralogy/Petrology of aggregates should also be tested to consider the differential polishing due to various mineral compositions.
- Extensive field testing (CTM and DFT) should be performed on various treatments to simulate better friction and texture values.
- Crash data and weather data should be added to the skid prediction model.

REFERENCES

AASHTO. (2010). *Highway Safety Manual* (Vol. 1st ed). Washington, D.C: American Association of State Highway and Transportation Officials.

Adam, J. F., & Gansen, E. (2001). *Performance of Poly-Carb, Inc. Flexogrid Bridge Overlay System*. Retrieved from Ames, IA: http://www.iowadot.gov/research/reports/Year/2003andolder/abstracts/mlr8604.pdf

Ahammed, A. M., & Tighe, S. L. (2007). Evaluation of Concrete Pavements Surface Friction Using LTPP Data: Preliminary Analysis and Texture Performance Models. *Transportation Research Board 86th Annual Meeting, No. 07-0727*.

Arambula, E., Estakhri, C., Epps-Martin, A., Trevino, M., Smit, A. d. F., & Prozzi, J. (2013). *Performance and Cost Effectiveness of Permeable Friction Course (PFC) Pavements*. Retrieved from College Station, TX: https://static.tti.tamu.edu/tti.tamu.edu/documents/0-5836-2.pdf

ASTM-E2157. E2157-15 "Standard Test Method for Measuring Pavement Macrotexture Properties Using the Circular Track Meter". In.

ASTM. (2007). *Annual Book of ASTM Standards, Vol. 04.03*. West Conshohocken, PA.

Bahar, G., C. Mollett, B. Persaud, C. Lyon, A. Smiley, T. Smahel, and H. McGee. (2004). Safety Evaluation of Permanent Raised Pavement Markers. *Transportation Research Board*.

Bischoff, D. L. (2008). *Investigative Study of Italgrip System*. Retrieved from Madison, WI: https://books.google.com/books/about/Investigative_Study_of_the_Italgrip_Syst.html?id=bLStPgAACAAJ

Bloem, D. L. (1971). Skid-Resistance: The Role of Aggregates and Other Factors. *National Sand and Gravel Association Circular 109,Silver Spring, MD*.

Bonneson, J., and M. Pratt. (2008). Procedure for Developing Accident Modification Factors from Cross-Sectional Data. *Transportation Research Record: Journal of the Transportation Research Board, National Research Council, Washington, D.C*, 40-48.

Brimley, B., & Carlson, P. (2012). *Using High Friction Surface Treatments to Improve Safety at Horizontal Curves*. http://d2dtl5nnlpfr0r.cloudfront.net/tti.tamu.edu/documents/TTI-2012-8.pdf

BRSQC. (2018). Bituminous Rated Source Quality Catalog. In.

Campbell, J. L., Board, N. R. C. T. R., Program, N. C. H. R., Highway, A. A. o. S., Officials, T., & Administration, U. S. F. H. (2012). *Human Factors Guidelines for Road Systems*: Transportation Research Board.

Cheung, J., Julian, F., & Moravec, M. (2014). Frequently Asked Questions about High Friction Surface Treatments. *Every Day Counts.* Retrieved from https://www.fhwa.dot.gov/everydaycounts/edctwo/2012/pdfs/fhwa-cai-14-019_faqs_hfst_mar2014_508.pdf

Choi, Y.-Y., Kho, S.-Y., Lee, C., & Kim, D.-K. (2015). Development of Crash Modification Factors of Alignment Elements and Safety Countermeasures for Korean Freeways. *Transportation Research Board*.

Choubane, B., Holzschuher, C. R., & S.Gokhale. (2004). Precision of Locked-Wheel Testers for Measurement of Roadway Surface Friction Characteristics. *Transportation Research Record: Journal of Transportation Research Board, 1869*(Transportation Research Board of National Academies, Washington, D.C.), 145-151.

Cooper, S. B., & Mohammad, L. N. (2004). *Novachip Surface Treatment: Six Year Evaluation, Theriot Canal Bridge–St. Charles Bridge*.

Correa, A. L., & Wong, B. (2001). *Concrete Pavement Rehabilitation – Guide for Diamond Grinding*. Retrieved from https://www.fhwa.dot.gov/pavement/concrete/diamond.pdf

Davis, R. M., G. W. Flintsch, I. L. K. Al-Qadi, and K. McGhee. (2002). Effect of Wearing Surface Characteristics on Measured Pavement Skid Resistance and Texture. *Transportation Research Board of the National Academies, Washington, D.C*.

Dewey, G. R., A. C. Robords, B. T. Armour, and R. Muethel. (2001). Aggregate Wear and Pavement Friction. *Transportation Research Board*(Transportation Research Board of the National Academies, Washington, D.C., 2001).

Do, M. T., Zahouani, H., & Vargiolu, R. (2000). Angular Parameter for Characterizing Road Surface Microtexture. *Transportation Research Record: Journal of Transportation Research Board, 1723*, 66-72.

Dr.R Gary Hicks, S. B. S., David.G.Peshkin. (2000, June 14). Selecting a Preventive Maintenance Treatment for Flexible Pavements, p. 87.
Elvik, R., and T. Vaa. (2004). *The Handbook of Road Safety Measures*. Oxford, United Kingdom.

Ergun, M., Iyinam, S., & Iyinam, A. F. (2005). Prediction of Road Surface Friction Coefficient Using Only Macrotexture and Microtexture Measurements. *Journal of Transportation Engineering, 131*(4), 311-319.

FHWA. (2011, June 24.2011). Retrieved from https://safety.fhwa.dot.gov/roadway_dept/horicurves/cmhoricurves/

FHWA. (2014, October 15 2014). Introduction to Crash Modification Factors. Retrieved from https://safety.fhwa.dot.gov/tools/crf/resources/cmfs/intro.cfm

Findley, D., C. Zegeer, C. Sundstrom, J. Hummer, and W. Rasdorf. (2012). Applying the Highway Safety Manual to Two-Lane Road Curves. *Journal of the Transportation Research Forum, 51 (2)*, 25-37.

Flintsch, G. W., León, E. d., McGhee, K. K., & Al-Qadi, I. L. (2003). Pavement Surface Macrotexture Measurement and Applications. *Transportation Research Board-2003, 1860*.

Forster, S. W. (1989). Pavement Microtexture and its Relation to Skid Resistance. *Transportation Research Record: Journal of Transportation Research Board, Transportation Research Board of National Academies Washington D.C., 1215*, 151-164.

Gilbert, T., Olivier, P., & Galé, N. (2004, September 2004). *Ultra Thin Friction Course: Five Years on in South Africa.* Paper presented at the 8th Conference on Asphalt Pavements for Southern Africa, Sun City, South Africa.

Gooch, J. P., V. V. Gayah, and E. T. Donnell. (2016). Quantifying the Safety Effects of Horizontal Curves on Two-Way, Two-Lane Rural Roads. (92), 71-81.

Gransberg, D. D. (2008). *Evaluate TXDOT Chip Seal Binder Performance Using Pavement Management Information System and Field Measurement Data*. Retrieved from Norman, OK:

Gransberg, D. D., & James, D. M. B. (2005). *NCHRP Synthesis 342: Chip Seal Best Practices*. Retrieved from Washington, D.C.: http://www.trb.org/Publications/Blurbs/155807.aspx

Hall, J. W., Glover, L. T., Smith, K. L., Evans, L. D., Wambold, J. C., Yager, T. J., & Rado, Z. (2006). *Guide for Pavement Friction*. Retrieved from National Cooperative Highway Research Program, Transportation Research Board:

Hall, J. W., Smith, K. L., Titus-Glover, L., Wambold, J. C., Yager, T. J., & Rado, Z. (2009). *Guide for Pavement Friction*. Retrieved from http://onlinepubs.trb.org/onlinepubs/nchrp/nchrp_w108.pdf

Harkey, D. L., Srinivasan, R., Baek, J., Council, F. M., Eccles, K., Lefler, N., . . . Bonneson, J. A. (2008). *Accident Modification Factors for Traffic Engineering and ITS Improvements*. Retrieved from Washington, D.C.:

Henry, J. J. (1986). Tire Wet-Pavement Traction Measurement: A State-of-the-Art Review. *ASTM Special Technical Publication 929: The Tire Pavement Interface*(ASTM, Philadelphia).

Herrington, P. R., Ball, G. F., & Patrick, J. E. (2004). Solutions for Improving Chipseal Life, Opus International Consultants Limited.

J.Taylor, G. (2014). Open graded friction courses.

Jayawickrama, P. W., Prasanna, R., & Senadheera, S. P. (1996). Survey of State Practices to Control Skid Resistance on Hot-Mix Asphalt Concrete Pavements. *Transportation Research Record, Transportation Research Board, TRB, National Research Council, Washington, D.C.*

Johnsen, W. A. (1997). *Advances in the Design of Pavement Surfaces.*

Julian, F., & Moler, S. (2008, July 2008). Gaining Traction in Roadway Safety. *Public Roads, 72*.

Kassem, E., Awed, A., Masad, E. A., & Little, D. N. (2013). Development of Predictive Model for Skid Loss of Asphalt Pavements. *Transportation Research Board*, 83-96.

Kassem, E., Scullion, T., Masad, E., Chowdhury, A., Liu, W., Estakhri, C., & Dessouky, S. (2012). *Comprehensive Evaluation of Compaction of Asphalt Pavements and Development of Compaction Monitoring System*. Retrieved from College Station, TX: http://tti.tamu.edu/documents/0-6992-2.pdf

Keith W. Anderson, J. S. U., Tim Sexton, Mark Russell, and, & Weston, J. (2012). *Evaluation of Long-Term Pavement Performance and Noise Characteristics of Open-Graded Friction Courses*.

Kokot, D. (2005). Evaluating Skidding Resistance in Slovenia. (Slovenian National Building and Civil Engineering Institute).

Kowalski, K. J. (2007). Influence of Mixture Composition on the Noise and Frictional Characteristics of Flexible Pavements. *Proquest*.

Krugler, P. E., Freeman, T. J., Wirth, J. E., Wikander, J. P., Estakhri, C. K., & Wimsatt, A. J. (2012). *Performance Comparison of Various Seal Coat Grades Used in Texas*. Retrieved from College Station, TX: http://d2dtl5nnlpfr0r.cloudfront.net/tti.tamu.edu/documents/0-6496-1.pdf

Kummer, H. W., & Meyer, W. E. (1963). Penn State Road Surface Friction Tester as Adapted to Routine Measurement of Pavement Skid Resistance. *Road Surface Properties*, *42nd Annual Meeting*.

Lawson, W. D. (2006). *Short Term Solutions to "Bleeding" Asphalt Pavements*. Retrieved from Lubbock, TX: http://library.ctr.utexas.edu/digitized/products/0-5230-P1-techmrt.pdf

Li, S., K. Zhu, S. Noureldin, and D. Harris. (2005). Identifying Friction Variations with the Standard Smooth Tire for Network Pavement Inventory Friction Testing. *Transportation Research Board*.

Linder, M., Kröger, M., Popp, K., & Blum, H. (2004). Experimental and Analytical Investigation of Rubber Friction. *XXI International Congress of Theoretical and Applied Mechanics, Warsaw, Poland*.

Long, K., Wu, H., Zhang, Z., & Murphy, M. (2014). *Quantitative Relationship between Crash Risks and Pavement Skid Resistance* (FHWA/TX-13/0-6713-1). Retrieved from Austin, TX:

Lord, D., Brewer, M., Fitzpatrick, K., Geedipally, S., & Peng, Y. (2011). *Analysis of Roadway Departure Crashes on Two-Lane Rural Roads in Texas* (FHWA/TX-11/0-6031-1). Retrieved from College Station, Texas:

Maher, M., C. Marshall, F. Harrison, K. Baumgaertner. (2005). *Context Sensitive Roadway Surfacing Selection Guide* (FHWA-CFL/TD-05-004a).

Mahmoud, E., & Masad, E. (2007). Experimental Methods for the Evaluation of Aggregate Resistance to Polishing, Abrasion. *Journal of Materials in Civil Engineering, 19*.

Mansour Solaimanian, S. S., Scott Milander, and Dennis Morian. (2016). *Evaluation of Thin Hot Mix Asphalt Overlay*.

Masad, E., Chowdhury, A., Kassem, E., & Aldagari, S. (2017). *Validation of Asphalt Mixture Pavement Skid Prediciton Model and Development of Skid Prediction Model for Surface Treatments*. Retrieved from College Station, TX: https://static.tti.tamu.edu/tti.tamu.edu/documents/0-6746-01-1.pdf

Masad, E., Rezaei, A., Chowdhury, A., & Freeman, T. J. (2010). *Field Evaluation of Asphalt Mixture Skid Resistance and Its Relationship to Aggregate Characteristics*. Retrieved from College Station, TX: http://tti.tamu.edu/documents/0-5627-2.pdf

McGee, H. W., and F. R. Hanscom. (2006). *Low-Cost Treatments for Horizontal Curve Safety* (FHWA-SA-07-002). Retrieved from Vienna, VA:

Meggers, D. (2015, January 2015). *Evaluation of High Friction Surface Locations in Kansas.* Paper presented at the 94th Annual Meeting of the Transportation Research Board, Washington, D.C.

Merritt, D. K., Lyon, C. A., & Persaud, B. N. (2015). *Evaluation of Pavement Safety Performance*. Retrieved from Washington, DC: http://www.fhwa.dot.gov/publications/research/safety/14065/14065.pdf

Moravec, M. (2013). High Friction Surface Treatments at High-Crash Curves. In *Arizona Pavements/Materials Conference*. Tempe, AZ.

Morian, D. A. (2011). *Cost Benefit Analysis of Including Microsurfacing in Pavement Treatment Strategies & Cycle Maintenance*. Retrieved from Harrisburg, PA: http://www.dot7.state.pa.us/BPR_PDF_FILES/Documents/Research/Complete%20Projects/Maintenance/080503%20Microsurfacing%20Final%20Report.pdf

Mukhopadhyay, B. T. W. a. D. A. (May 2016). *Alternative Aggregates and Materials for High Friction Surface Treatments*.

Neuman, T. R., Pfefer, R., Slack, K. L., Hardy, K. K., Council, F., McGee, H., . . . K. Eccles, K. A. (2003). *A Guide for Addressing Run-Off-Road Collisions* (Vol. 6). Transportation Research Board, Washington, DC: NCHRP Report 500.

Newcomb, D. E. (2009). *Thin Asphalt Overlays for Pavement Preservation*. Retrieved from Lanham, MD: http://www.asphaltpavement.org/images/stories/is-135.pdf

NHI, N. H. I. (2013). *Preventive Maintenance Treatment, Timing, and Selection*. Retrieved from Washington, DC:

NHTSA. 2009. "Traffic Safety Facts, D. (2009). Retrieved January 22, 2018 https://crashstats.nhtsa.dot.gov/Api/Public/ViewPublication/811161

Noyce, D. A., Bahia, H. U., Yambó, J. M., & Kim, G. (2005). *Incorporating Road Safety into Pavement Management: Maximizing Asphalt Pavement Surface Friction for Road Safety Improvements*.

Pashindu, H. R., Fwa, T. F., & Ong, G. P. (2010). Evaluation of Aircraft Landing Overrun Risk. *7th International Conference on Road and Airfield Pavement Technology, Bangkok, Thailand*.

Peshkin, D. G., T.E. Hoerner, and K.A. Zimmerman. (2004). *Optimal Timing of Pavement Preventive Maintenance Treatment Applications*. Retrieved from Washington, D.C:

PIARC. (1995). International PIARC Experiment to Compare and Harmonize Texture and Skid Resistance Measurements. (PIARC Technical Committee on Surface Characteristics (C1), Paris, France).

Pierce, L. M., & Kebede, N. (2015). *Chip Seal Performance Measures – Best Practices*.

Pratt, M. P., and J. A. Bonneson. (2008). Assessing Curve Severity and Design Consistency Using Energy- and Friction-Based Measures. *Transportation Research Record (2075),* 8-15.

Pratt, M. P., Geedipally, S. R., Pike, A. M., Carlson, P. J., Celoza, A. M., & Lord, D. (2014). *Evaluating the Need for Surface Treatments to Reduce Crash Frequency on Horizontal Curves*. Retrieved from College Station, TX: https://static.tti.tamu.edu/tti.tamu.edu/documents/0-6714-1.pdf

Prowell, B. D., Zhang, J., & Brown, E. R. (2005). Aggregate Properties and the Performance of Superpave-Designed Hot Mix Asphalt. *Transportation Research Board, 539*.

Roberts, F. L., Kandhal, P. S., Brown, E. R., Lee, D.-Y., & Kennedy, T. W. (1996). Hot Mix Asphalt Materials, Mixture Design and Construction. Second edition. *TRID*.

Roe, P. G., Parry, A. R., & Viner, H. E. (1998). *High and Low Speed Skidding Resistance: The Influence of Texture Depth*. Retrieved from Berkshire, U.K:

Rogers, C. (1991). Laboratory Tests for Predicting Coarse Aggregate Performance in Ontario. *Advances in Aggregate and Armourstone Evaluation, 13*.

Romero, P., & Anderson, D. (2004). *Life Cycle of Pavement Preservation Seal Coats*.

Saito, K., Horiguchi, T., Kasahara, A., Abe, H., & Henry, J. J. (1996). Development of Portable Tester for Measuring Skid Resistance and Its Speed Dependency on Pavement Surfaces. *Transportation Research Record, National Research Council, Washington, D.C, 1536*.

Satterthwaite, S. (1976). An Assessment of Seasonal and Weather Effects on the Frequency of Road Accidents in California. *Elsevier, Accident Analysis & Prevention, Vol. 8*, 87-96.

Schneider, W. H., P. T. Savolainen, and K. Zimmerman. (2009). Driver Injury Severity Resulting from Single-Vehicle Crashes Along Horizontal Curves an Rural Two-Lane Highways. *Transportation Research Record (2102)*, 85–92.

Senadheera, S. P., Henderson, R. B., Surles, J. G., & Lawson, W. D. (2013). *Implementing the Ultra-High Pressure Water Cutter for Roadway Maintenance Applications*. Retrieved from Lubbock, TX:

Seneviratne, P. N., & Bergener, J. M. (1994). *Effects of Aggregate Seal Coats on Skid Index Numbers & Accident Rates of Low Volume Roads in Utah*.

Shafii, M. A. B. (2009). *Skid Resistance and the Effect of Temperature*. Retrieved from Malaysia:

Smith, R. N., & Elliott, L. E. (1975). *Evaluation of Minor Improvements (Part 8), Grooved Pavement* (CADOTTR2152-11-75-01).

Srinivasan, R., Baek, J., Carter, D., Persaud, B., Lyon, C., Eccles, K. A., . . . Lefler, N. X. (2009). *Safety Evaluation of Improved Curve Delineation* (FHWA-HRT-09-045). Retrieved from University of North Carolina, Chapel Hill, NC:

Stubstad, R., Darter, M., Rao, C., Pyle, T., & Tabet, W. (2005). *The Effectiveness of Diamond Grinding Concrete Pavements in California*. Retrieved from California:

Sullivan, B. W. (2005). Development of a Fundamental Skid Resistance Asphalt Mix Design Procedure. *In Proceedings, International Conference on Surface Friction,Christchurch,New Zealand*, 170.

Taneerananon, P., & Yandell, W. O. (1981). Microtexture Roughness Effect on Predicted Road/Tire Friction in Wet Condition. *69*, 321-337.

Tate, T. R., & Clark, T. M. (2004). *Thin Hot Mix Asphalt Overlays and SR 164 Case Study*.

Torbic D. J., J. M. H., C. D. Bokenkroger, K. M. Bauer, D. W. Harwood, D. K. Gilmore, J.M. Dunn, J. J. Ronchetto, E. T. Donnell, H. J. Sommer, P. M. Garvey, B. Persaud, and C.Lyon. (2009). *Guidance for the Design and Application of Shoulder and Centerline Rumble Strips*: Transportation Research Board.

Torbic, D. J., Harwood, D. W., Gilmore, D. K., Pfefer, R., Neuman, T. R., Slack, K. L., & Hardy, K. K. (2004). *A Guide For Reducing Collisions On Horizontal Curves*: Transportation Research Board.

Tsyganov, A. R., Machemehl, R. B., & Warrenchuk, N. (2009). Driver Performance and Safety Effects of Edge Lines on Rural Two-Lane Highways. *Transportation Research Board (88th Annual Meeting), 09-0751*.

Tsyganov, A. R., R. B. Machemehl, and N. Warrenchuk. (2009). *Driver Performance and Safety Effects of Edge Lines on Rural Two-Lane Highways* (FHWA/TX-07/0-5090-2).

Wade, M., R.l DeSombre, & Peshkin, a. D. G. (2001). *High Volume/High Speed Asphalt Roadway Preventive Maintenance Surface Treatments*. Retrieved from South Dakota:

Walden, T. D., D. Lord, M. Ko, S. Geedipally, and L. Wu. (2014). *Developing Methodology for Identifying, Evaluating, and Prioritizing Systemic Improvements*. Retrieved from College Station, TX:

Walubita, L., & Scullion, T. (2008). *Thin HMA Overlays in Texas: Mix Design and Laboratory Material Property Characterization*. Retrieved from College Station, TX:

Waters, J. (2011). *High Friction Surfacing Failure Mechanisms*. Retrieved from Gold Coast, Australia: https://s3.amazonaws.com/media.atssa.com/Resources/High+Friction+Surfacing/Waters+-+High+Friction+Surfacing+Failure+Mechanisms.pdf

Watters, J. C. (2006). Ultra Thin Asphalt a Cost Effective Treatment with Texture *NZIHT 2006 Conference Recycled asphalt and porous pavements - Environmental, Social and Cost Advantages*.

William "Bill" King, J., Md Sharear Kabir, Samuel B.Cooper,Jr., Christopher Abadie. (2013). *Evaluation of Open Graded Friction Course (OGFC) Mixtures* (FHWA/LA.13/513).

Wilson, B. T., & Mukhopadhyay, A. K. (2016). *Alternative Aggregates and Materials for High Friction Surface Treatments*. Retrieved from College Station, TX: http://www.fdot.gov/research/completed_proj/summary_SMO/FDOT-BDR74-977-05-rpt.pdf

Wilson, B. T., Scullion , T., & Estakhri, C. (2013). *Design and Construction Recommendations for Thin Overlays in Texas*. Retrieved from College Station, TX: http://d2dtl5nnlpfr0r.cloudfront.net/tti.tamu.edu/documents/0-6615-1.pdf

Wilson, B. T., Scullion, T., & Faruk, A. (2015). *Evaluation of Design and Construction Issues of Thin HMA Overlays*. Retrieved from College Station, TX: http://ntl.bts.gov/lib/54000/54900/54960/0-6742-1.pdf

Wu, Z., Groeger, J. L., Simpon, A. L., & Hicks, R. G. (2010). *Performance Evaluation of Various Rehabilitation and Preservation Treatments*. Retrieved from https://www.fhwa.dot.gov/pavement/preservation/pubs/perfeval/perfeval.pdf

Yandell, W. O. (1971). A New Theory of Hysteretic Sliding Friction. *17*.

Zegeer, C. V., J. R. Stewart, F. M. Council, and D. W. Reinfurt. (1991). Safety Effects of Geometric Improvments on Horizontal Curves. *Transportation Research Record (1356), UNC-HSRC-91*.

APPENDIX A

Table 13: Literature on Crash Modification Factors of Pavement Treatments

Year	Study Scope	Section Type	Crash Type	CMF	Reference
High Friction Surface Treatments					
2015	8 states, 57 sections, sufficient before-after data, and reference sites.	Ramps	Wet	0.139	(Merritt et al., 2015)
			Total	0.653	
		Curves	Wet	0.481	
			Total	0.759	
2013	Kentucky, 43 sections (Overlaps with Merritt'15)	Curves	Wet	0.14	(Merritt et al., 2015)
			Total	0.27	
		Ramps	Wet	0.15	
			Total	0.34	
2016	Florida, 40 sections	Tight curves and ramps	Wet	0.25	(Mukhopadhyay, May 2016)
			Total	0.68	
		Wide curves and tangents	Wet and Total	Not significant	
NCHRP		High wet-weather accident locations	Wet	0.76	(Harkey et al., 2008)
			Total	0.43	
2012	Lit. review		Wet	0.50	(Brimley & Carlson, 2012)
			Total	0.80-0.70	
2008	Wisconsin	-	-	0.07	(Bischoff, 2008)
	Michigan, 4 sites, 1-yr. (Overlaps with Merritt'15)	-	-	0.40	(Moravec, 2013)

Table 13 (continued)

Year	Study Scope	Section Type	Crash Type	CMF	Reference
Seal Coats					
1995	NYDOT (Thin Overlays)-	36 Sites, Long Island	Wet	0.50	(Merritt et al., 2015)
1997			Total	0.80	
2015	4 States, 2557 miles	Multilane	Wet	0.775	(Merritt et al., 2015)
			Total	1.147	
1990	Utah DOT, 34-one-mile long sections	Non-Interstate, low volume roadways	Wet	0.61	(Seneviratne & Bergener, 1994)
			Dry	0.55	
Thin Asphalt Overlays					
2015	California and North Carolina	Freeway	Wet	0.91	(Merritt et al., 2015)
			Total	1.0	
		Multilane	Wet	0.91	
			Total	1.05	
		Two-Lane	Wet	1.15	
			Total	1.19	
Permeable Friction Course					
2009	Louisiana Police Report, U.S 71	I-20 (study of one application)	Wet	0.24	(William "Bill" King, 2013)
			Total	0.43	
				Decreasing over 4 years	(Merritt et al., 2015)
Abrading and Texturing					
1990	3 year before and 1-yr after, California	Grooving	Wet	0.28	(Correa & Wong, 2001)
1975	Freeways, Los Angeles	Grooving	Wet	0.31	(Smith & Elliott, 1975)

Table 14: **Literature Review on Skid Resistance of Pavement Treatments**

Study Year	Study Scope	Measurement Type	Initial Value	Years Later	Later Value	Reference
High Friction Surface Treatment						
2008	Wisconsin	SN	73	5	59	(Bischoff, 2008)
2016	Florida	SN40R	>70	6	63-78	
2001	Iowa bridge deck	SN	67.5	4	64.5	(Adam & Gansen, 2001)
2015	Kansas, flint aggregate	SN	88	4	54	(Meggers, 2015)
Seal Coat						
	Utah	SN_R	Avg. (range)	6	Avg. (range)	
Thin Overlay						
2004	VDOT	SN	36.1(before treatment)	1	46.7(after treatment)	(Tate & Clark, 2004)
	Penn DOT	μ from DFT	0.60-0.62	-	-	(Mansour Solaimanian, 2016)
2016	Penn DOT	SN40	30(before treatment)	-	50(after treatment)	(Mansour Solaimanian, 2016)
		MPD (CTM test)	0.69	-	-	
Permeable Friction Course						
2012	WSDOT	FN40R OGFC-HMA	54	3	51	(Keith W. Anderson & Weston, 2012)

Table 15: Literature Review on Service Life of Pavement Treatments

Study Year	Study Scope	Years	Comment	Reference
High Friction Surface Treatment				
2014	International	7-12	-	(Cheung et al., 2014)
	Bridge decks (some)	>15	-	
-	Vendor report	5-8	15,000 veh/day	-
-	Vendor report	Up to 5	50,000 veh/day	-
-	Michigan bridge decks	12-15	Includes site with 48,000-62,000 ADT	-
2016, 2011	New Zealand, Florida	<1	Poor construction practices	(Waters, 2011; Wilson & Mukhopadhyay, 2016)
Seal Coat				
2012	Survey of 22 State DOTs	6.5 (3-15)	-	(Krugler et al., 2012)
	New York	3-4	-	-
	Washington	5-7	-	-
	Texas	4-7	5,000 veh/day	-
2013	-	3-15	In general	(NHI, 2013)
		4-6	Single	
		5-7	Double	
-	Survey of 31 U.S State Highway agencies and 6 Canadian agencies from Ministry of Transportation	5.6-7.8	New construction	(Pierce & Kebede, 2015)
		6-7.5	Over chip seal	
		6.5-7.4	Over existing asphalt	
		8.2-10.2	Grade 4	(Herrington, Ball, & Patrick, 2004)
		5.4-8.1	Grade 3	
		5.9-7.7	Grade 2	
2004	Utah	27	Skid function only	(Romero & Anderson, 2004)

Table 15 (continued)

Study Year	Study Scope	Years	Comment	Reference
Thin Overlay				
2000	-	4-6	-	(Dr.R Gary Hicks, 2000)
2006	-	5-16	-	(Watters, 2006)
2008	Texas	8-15	-	(Walubita & Scullion, 2008)
2004	NCDOT and VDOT	3 minimum	-	(Tate & Clark, 2004)
	-	8+	Replacement	
2009	-	10+	Over flexible	(Newcomb, 2009)
		6-10	Over rigid	
Permeable Friction Course				
	Ultra-thin PFC	7+		(Gilbert, Olivier, & Galé, 2004; Maher, 2005; Peshkin, 2004)
2014		10-15	-	(J.Taylor, 2014)
Texturing				
	SHRP 2	8	Diamond grinding	(Merritt et al., 2015)
2005	California	16-17	Diamond grinding	(Stubstad, Darter, Rao, Pyle, & Tabet, 2005)
	Oklahoma DOT	2	Abrading and shotblasting	ODOT
2015		1	Milling on seal coats	-
		1.5	Milling on HMA	

Table 16: Literature Review on Unit Cost of Pavement Treatments

Study Year	Study Scope	$/sq-yd	Comments	Reference
High Friction Surface Treatment				
2014	NA	$25-$35	Historic	(Cheung et al., 2014)
	NA	$19-$21	Rolling several projects together	
2016	Florida, 40 sections	$34 ($26-$40)	Unit cost	(Wilson & Mukhopadhyay, 2016)
		$59 ($36-$113)	Comprehensive unit cost	
Seal Coat				
2008	Cost Index Number Analysis	$0.82	Emulsion-SC	(D. D Gransberg, 2008)
		$0.92	Asphalt-SC	
2011		$1-$2		(Morian, 2011)
2005		$0.70-$1.25	Single	(Maher, 2005)
		$1.25-$2.50	Double	
Thin Overlay				
2014		$2.07	$14,600 per lane mile	(NCHRP Synthesis 464, 2014)
2000		$1.75		(Dr.R Gary Hicks, 2000)
2000?		$1.75	$25/ton, 1.25-inch thick	(Dr.R Gary Hicks, 2000)
Permeable Friction Course				
2001				(Peshkin, 2004)
2004				(Maher, 2005)
		$7.34	NovaChip	(Cooper & Mohammad, 2004)
		$12.43	Includes 2" SMA	(William "Bill" King, 2013)

Table 17: Site List: (a) PFCs, (b) Seal Coats, (c) HMA, (d) HFST and High-Pressure Water Cutting

ID	SECTION LABEL	Surface Type	Surface Type 2	Const Date	CSJ	Proj BTRM	Proj ETRM	From	To	New	Use in query?	Confirmed Surface	AADT	Agg Type
1	PFC-US 59-Wharton-Yoakum (Kendelton)	PFC		Jun-07	0089-06-076	?	?			Y	Y	Aug-17	13000	Limestone
2	PFC-US 59-Wharton-Yoakum (Hillje)	PFC		Jun-07		588+1.720	594+1.773	LP 524 NORTH OF HILLJE	0.14 MI. N. OF FM 647 (NB LN), ETC	Y	Y	Aug-17		Unknown
3	PFC-SH 288-Brazoria-Houston	PFC		Oct-06	0598-02-043	484+0.730	498+1.955	FM 2234	HAYES CREEK	N	Y	Feb-17	14160	Granite + Limestone
4	PFC-SH 288-Brazoria-Houston-A	PFC		Jul-17		484+0.730	498+1.955	FM 2234	HAYES CREEK	Y	Y	Aug-17		Unknown
5	PFC-SH 288-Brazoria-Houston-B	PFC		Jun-10						Y	Y	Aug-17		Unknown
6	PFC-US 290-Bastrop-Austin	PFC		Apr-07	0114-06-031	626+0.083	632+0.000	1.5 MI W OF FM 2104	LEE C/L	N	Y	Jun-11	16300	Sandstone
7	PFC-IH 30-Hopkins-Paris	PFC	TBPFC	May-06	0010-02-079	127+0.133	134+0.605	LOOP 301	HOPKINS/FRANKLIN COUNTY	N	Y	Dec-15	12300	Sandstone
8	PFC-SH 6-Robertson-Bryan	PFC		May-09	0049-06-061	544+0.922	554+0.445	GRASSY CREEK	NOVASOTA RIVER	Y	Y?	Aug-17	4800	Sandstone + Limestone
9	PFC-IH 20-Taylor-Abilene	PFC		Jun-05	0006-05-XXX	279-0.44	283+0.463	NEAR SPINKS ROAD IN	THE INTERCHANGE @ US 83 /	N	N	Unknown	10335	Limestone
10	PFC-US 83-Taylor-Abilene	PFC		Sep-05	0033-06-097	322+0.75	328+0.065	NEAR FM 2404	US 277	Y	Y	Apr-16	18690	Limestone
11	PFC-SH 240-Wichita-Wichita Falls	PFC	UTBHMWC	May-08	0156-03-044	468+0.489	470+1.436	WICHITA RIVER	BU 287J	N	Y	Jul-15	3750	Siliceous + Limestone
12	PFC-SH 6-McLennan-Waco	PFC		Aug-05	0049-01-085	570+0.454	508-0.716	BU 77-L	SH 164	Y	N	Nov-11	8550	Limestone
13	PFC-US 281-Bexar-San Antonio	PFC		May-05	0521-04-223	534+0.361	530+1.996	BASS RD	0.40 MILES N OF HILDEBRAN	N	Y	Jan-15		Traprock
14	PFC-SH 6-Waller-Houston	PFC		Jul-05	0050-04-025	626+1.074	632+3.108	GRIMES COUNTY LINE	US 290	Y	Y	Feb-17	10000	Unknown
15	PFC-IH 37-San Patricio-Corpus Christi	PFC		May-04	0074-05-089	-	-	0.5 MI S OF MEDINA R	MEDINA RIVER	N	Y	Jun-13		Limestone/Gravel
16	PFC-IH 37-Nueces-Corpus Christi	PFC		Apr-04	0074-06-197	0+0.000	16+0.644	0.5 MI S OF MEDINA R	MEDINA RIVER	N	Y	Jan-17		Limestone
17	PFC-US 77-San Patricio-Corpus Christi	PFC		Jul-09	0372-01-092	656+1.96	654+0.572	1.532 MILES S. OF CR 1	68 FT S. OF COOPER ST.	N	Y	Jan-17	14500	Limestone/Gravel
18	PFC-IH 35-McLennan-Waco	PFC		May-03	0015-01-164	340+0.052	343+0.622	CRAVEN AVE	2.57 MILES SOUTH OF CRAVE	N	Y	Nov-11	41385	Rhyolite
19	PFC-IH 20-Van Zandt-Tyler	PFC		Jun-08	0495-02-057	524+0.577	527+0.476	1.3 MI E OF SH 64, E	SH 19, N OF CANTON	Y	Y	Aug-17	17525	Unknown
20	PFC-IH 20-Smith-Tyler	PFC		Aug-09	0910-00-085	534+0.787/571	597+0.000/580	2.5 MI W OF FM 773, E	0.4 MI W OF US 259	Y	Y	Aug-17	14980	Sandstone
21	PFC-US 281-Bexar-San Antonio	PFC		Sep-06	0073-08-150	534+0.361	536+0.515	0.4 MI N OF HILDEBRA	PEARL PARKWAY	N	Y	Jul-16	73415	Sandstone/Limestone
22	PFC-SH 6-Fort Bend-Houston	PFC	TBPFC	Apr-05	1685-06-027	678+2.323	684+1.127	HARRIS C/L	US 90A	N	Y	Apr-14	34000	Quartzite
23	PFC-US 287-Clay-Wichita Falls	PFC	UTBHMWC	Aug-05	0224-01-054	362+0.916	366+0.622	NEAR US 82 OVERPASS	APPROX. 0.8 MILES EAST OF	N	Y	Dec-11	8335	Granite/Dolomite
24	PFC-US 82-Clay-Wichita Fals	PFC	UTBHMWC	Aug-05	0044-02-072	530+0.678	542+0.895	-	-	N	Y	Nov-09	9290	Granite/Dolomite
25	PFC-SL 473-Wichita-Wichita Falls	PFC	UTBHMWC	May-08	0249-11-009	192+0.854	194+1.673	US 287 NORTH FRONT/	FM 369	N	Y	Feb-17		Granite/Dolomite
26	PFC-US 281-Hidalgo-Pharr	PFC		May-04	0255-08-091	778+0.3	782+0.4	SH 495	TRENTON ROAD	N	Y	Jun-11	39945	Gravel
27	PFC-US 90-Waller-Houston	PFC		Mar-04	0271-09-017	794-0.723	794+1.327	IH 10, EAST OF PEACH I	FM 359	N	Y	Feb-10		Sandstone
28	PFC-SL 289-Lubbock-Lubbock	PFC		Oct-10	0783-01-093	312+0.364	308+0.128	FM 1730 (SLIDE RD)	IH 27	N	Y	Feb-17		Gravel/Limestone
29	PFC-US 69-Cherokee-Tyler	PFC		Apr-07	0199-01					N	N			
30	PFC-US 69-Cherokee-Tyler	PFC		Apr-07	0199-01					N	N			
31	PFC and dense hot mix -SH 110-Smith-Tyler	PFC and dense hot mix		Apr-10						N	N			
32	PFC and dense hot mix -SH 110-Smith-Tyler	PFC and dense hot mix		Apr-10						N	N			

(a)

Table 17 (continued)

ID	SECTION LABEL	Surface Type	Surface Type 2	Const Date	CSJ	Proj BTRM	Proj ETRM	From	To	New	Use in query?	Confirmed Surface	AADT	Agg Type
33	Seal Coat-US 77-Cameron-Pharr	Seal Coat	Grade 3	May-13		786+0.0	778+0.0			N	Y	Jan-16		Limestone
34	Seal Coat-US 281-Hidalgo-Pharr	Seal Coat	Grade 3	May-13	0255-07	766+0.5	766+0.0			N	Y	Jan-17		Limestone
35	Seal Coat-US 281-Brooks-Pharr	Seal Coat	Grade 3, Pre	May-11		752+0.0	735+0.0			N	Y	Jan-17		Limestone
36	Seal Coat-US 281-Brooks-Pharr	Seal Coat	Grade 3	Sep-11		722+0.0 (at least)	716+0.0 (at least)			N	Y	Jun-16		Limestone
37	Seal Coat-US 377-Hood-Dallas-FW	Seal Coat	Grade 3	Jul-10	0080-04	328+1.5	322+0.00	SH 171		Y	Y	Jan-17	24000	Limestone
38	Seal Coat-SH 199-Parker-Dallas-FW	Seal Coat	Grade 3	Jul-11	171-03	534+0.00	544+0.00	Wise Co Line		N	Y	Mar-15	3700-9100	Limestone
39	Seal Coat-US 377-Tarrant-Dallas-FW	Seal Coat	Grade 3	Jul-10	0080-07	312+0.00	306+0.00	Parker Co Line		N		2016/Late 2015	19700-2900(	Limestone
40	Seal Coat-US 67-Coleman-Brownwood	Seal Coat	Grade 4	Jul-10		586+0.000	592+1.917			Y	Y	Oct-16		Limestone
41	Seal Coat-US 67-Brown-Brownwood	Seal Coat	Grade 4	Jul-11		580+1.223	586+0.000			Y	Y	Oct-16		Limestone
42	Seal Coat-US 183-Eastland-Brownwood	Seal Coat	Grade 4	Jul-12	0127-01	330+0.461	338+0.570			Y	Y	Jan-15		Limestone
43	Seal Coat-US 377-Brown-Brownwood	Seal Coat	Grade 4	Jul-12	0128-01	427-0.088	432+0.108			Y	Y	Jul-15		Limestone
44	Seal Coat-US 90/IH 10-Bexar-San Antonio	Seal Coat	Grade 4	Jun-13	0024-07-057	H 410 TRM 563+0.	L 1604 TRM 560+0.5			N	Y	Jan-17		Limestone
45	Seal Coat-FM 1518-Bexar-San Antonio	Seal Coat	Grade 3	Jun-13	0465-02-023	FM 78, 490+2.0	FM 1346, 502+0.0			Y	Y	Aug-17		Sandstone
46	Seal Coat-SH 16-Atascosa-San Antonio	Seal Coat	Grade 4	Jun-12	0613-02-056	ar Co lineTRM 61	M 476 TRM 626+1.0			N	Y	Jan-17		Traprock
47	Seal Coat-SH 16-Atascosa-San Antonio	Seal Coat	Grade 3	Jun-12	0517-01-042	TRM 638	644			N	Y	Feb-14		Limestone? Trap Rock?
48	Seal Coat-SH 36-Austin-Yoakum	Seal Coat	Grade 3	Aug-08	N/A	613				Y	N	Aug-17		Limestone
49	Seal Coat-US 59-Angelina-Lufkin	Seal Coat	Grade 3	Jun-10	0176-03	400+0.0	402+1.2			N	Y	May-16		Traprock
50	Seal Coat-US 69-Angelina-Lufkin	Seal Coat	Grade 4	Jun-12	0200-01-080	424+1.442	426+1.442			Y	Y	Jul-16		Lightweight (Expanded Sh
51	Seal Coat-US 287-Trinity-Lufkin	Seal Coat	Grade 4	Jun-13	0340-02-024	650+1.76	660+1.2			Y	Y	Aug-17		Lightweight (Expanded Sh
52	Seal Coat-FM 2213-San Augustine-Lufkin	Seal Coat	Grade 5	Jun-12	1680-02-016	344+0.53	348+0.1			Y	Y	Aug-17		Lightweight (Expanded Sh
53	Seal Coat-US 59-Shelby-Lufkin	Seal Coat	Grade 4	Jun-12	0175-05-042	338+1.1	344+0.18			Y	Y	Oct-16		Sandstone
54	Seal Coat-LP 338-Ector-Odessa	Seal Coat	Grade 4	Jun-12	2224-01-079	52+.02 US 38	256+0.0 IH 20			N	Y	Feb-17		Rhyollite
55	Seal Coat-US 385-Crane-Odessa	Seal Coat	Grade 4	Jun-09		370+0.0 Ector Co l	380+0.0			N	Y	Feb-17		Limestone
56	Seal Coat-US 385-Ector-Odessa	Seal Coat	Grade 3	Jun-10		TRM 346	TRM 348			N	Y	Feb-17		Limestone
57	Seal Coat-SH 82-Jefferson-Beaumont	Seal Coat	Grade 4	Sep-10	2367-01-036	460+0.0	468+0.0			N	N	Oct-14		Lightweight (Expanded Sh
58	Seal Coat-FM 365-Jefferson-Beaumont	Seal Coat	Grade 4	Jul-13	0932-01-112	52+ 1.244 SH 12	766+1.592 SP 93			N	Y	Jan-17		Lightweight (Expanded Sh
59	Seal Coat-FM 105-Orange-Beaumont	Seal Coat	Grade 4	Jul-13	0710-02-063	8 2.24 mi north of	438+1.598 FM 1132			N	Y	Jan-17		Lightweight (Expanded Sh
60	Seal Coat-US 80-Harrison-Atlanta	Seal Coat	Grade 4	Jun-12	0096-10	TRM 824 +0.0	826+0.5			Y	Y	Aug-17		Lightweight (Expanded Sh
61	Seal Coat-SH 7-Houston-Lufkin	Seal Coat	???	Aug-17		?	?	It's really long		Y	N	Aug-17		Lightweight (Expanded Sh
62	Seal Coat-US 59-Cass-Atlanta	Seal Coat	Grade 3, Pre	Jun-13	0218-04-111	TRM 238	TRM 236			N	Y	Sep-16		Gravel
63	Seal Coat-SH 77-Cass-Atlanta	Seal Coat	Grade 4, Pre	Jun-12	0278-01	TRM 746	TRM 744			N	Y	Jan-15		Sandstone
64	Seal Coat-SH 77-Cass-Atlanta	Seal Coat	Grade 4, Pre	Jun-13	0277-02	TRM 720+0.986	TRM 728+0.974			N	Y	Feb-15		Gravel
65	Seal Coat-US 59-Panola-Atlanta	Seal Coat	Grade 3	Jul-12						Y	N	Aug-17		Sandstone

(b)

Table 17 (continued)

ID	SECTION LABEL	Surface Type	Surface Type 2	Const Date	CSJ	Proj BTRM	Proj ETRM	From	To	New	Use in query?	Confirmed Surface	AADT	Agg Type
66	HMA-US 77-Kennedy-Pharr	HMA	Type D	Feb-13		758+0.0	750+0.0 (at least)	754-0.1		N	Y	Nov-16		Gravel
67	HMA-US 281-Hidalgo-Pharr	HMA	Type D	Aug-11		772+0.5	768+0.5	772-0.1		N	N	Jan-17		Gravel
68	HMA-US 259-Rusk-Tyler	HMA	Type C	Feb-07		338+0.0	334+0.0			N	Y	Feb-15		Sandstone + Limestone
69	HMA-FM 973-Travis-Austin	HMA	Type C	Jan-12		448+1.0	452+0.0	452		Y	Y	Aug-17		Limestone
70	HMA-SH 71-Travis-Austin	HMA	TOM	Jul-13		584+0.0	588+0.0	584+1.0		Y	Y	Aug-17		Sandstone + Limestone
71	HMA-FM 3238-Travis-Austin	HMA	TOM	Jul-13		514+0.5	522+0.0	514+0.5		Y	Y	Aug-17		Sandstone + Limestone
72	HMA-IH 45-Leon-Bryan	HMA	Type C	Aug-08		164+0.0	167+0.7	167+0.6		Y	Y	Aug-17		Sandstone + Silliceous Riv
73	HMA-IH 10-Austin-Yoakum	HMA	Type D	Jul-11	0271-02-057	710+1.5	726+1.5	714		Y	Y	Feb-17		Dolomite-Limestone
74	HMA-SH 36-Austin-Yoakum	HMA	Type D	Jul-06	0187-04-028	612+1.0	618+1.0	612+1.1		N		2016		Limestone
75	HMA-SH 7-Houston-Lufkin	HMA	Type D	May-13	0336-02-024	694	702	698+0.8		N	Y	Sep-16		Granite + Limestone
76	HMA-IH 35-Webb-Laredo	HMA	SMA	Jul-03	0018-06-147	7+0.868	12+0.9	12.7		N	Y	Feb-17		Traprock + Gravel
77	HMA-IH 35-La Salle-Laredo	HMA	SMA	Jul-03		TRM 65	TRM 69+0.5			N	N	2014		Basalt + Traprock
78	HMA-IH 35-La Salle-Laredo	HMA	SMA	Jul-04	0018-02-049	49+0.431	53+0.42	TRM 50		N	Y	May-14		Traprock + Limestone
79	HMA-US 385-Ector-Odessa	HMA	CMHB-F	Oct-05	0229-01-028	56+0.76 IH 2	+0.0 Crane Co L	370-0.1		N	Y	Dec-09		Rhyollite and LS Scrn (?)
80	HMA-IH 20-Midland-Odessa	HMA	SP-D	Jul-12	0005-15-081	+0.7 Martin Co L	44-0.281 Bus IH 20			N	Y	Feb-17		Rhyollite and LS (dolomite
81	HMA-IH 20-Martin-Odessa	HMA	SP-C	Aug-12	0005-04-068	0.228 Howard Co	58+0.981 Bus IH 2	162		N	Y	Feb-16		Rhyollite and LS (dolomite
82	HMA-IH 20-Midland-Odessa	HMA	SP-D	Jul-13	0005-14-077	6+0.141 SH 3	+0.467 Ector Co Li	128+0.7		N	Y	Apr-16		Rhyollite and LS (dolomite
83	HMA-IH 10-Jefferson-Beaumont	HMA	SMA-D	Jul-09	0739-02-139	839+0.405	848+0.772	844+0.2		N	Y	Jan-17		Granite + ?
84	HMA-US 90-Jefferson-Beaumont	HMA	SMA	Jun-13	0028-06-074	900+1.061 FM 100	902+0.260 FM 365	902-0.25		N	Y	Jan-17		Sandstone + Limestone
85	HMA-SH 82-Jefferson-Beaumont	HMA	SMA	Apr-13	0508-05-029	54-0.513 SH 7	6+0.496 SH	454+0.5		N	Y	Jan-17		Granite + ?
86	HMA-Loop 207-Chambers-Beaumont	HMA	Type D	May-13	0389-10-011	462-0.068	462+0.602	462+0.35		N	Y	Feb-17		Sandstone + Limestone
87	HMA-US 59-Panola-AtlantaS Carthage	HMA	Type D	Apr-11	0063-05-033	TRM 324+3.02 (CL)	316+1.0	TRM 320+1.0		Y	Y	Oct-16		Quartzite
88	HMA-US 59-Panola-AtlantaN Carthage	HMA	Type D	Jun-11	0063-03-057	TRM 310+0.2	304+.4	TRM 311		Y	Y	Aug-16		Quartzite
89	HMA-US 59-Panola-Atlanta	HMA	CMHB-F	Aug-05	0063-10-011	304+.4	300 +.0	TRM 302-0.2		N	Y	Nov-13		Quartzite
90	HMA-IH 30-Bowie-Atlanta	HMA	SMA-F	Jul-10	0610-06-076	208+1.0	TRM 206	TRM 207+0.5		N	Y	May-13		Sandstone + Gravel
91	HMA-IH 20-Harrison-Atlanta	HMA	SMA-C	Jul-04		632+0.19	636+0.11			N	Y	Jan-13		Quartzite
92	HMA-US 271-Camp-Atlanta	HMA	CMHB-F	Jul-08	0248-02-053	TRM 262	TRM 266+0.3	TRM 262+0.3		N	N	Aug-16		Siliceous Gravel
93	HMA-US 59-Wharton-Yoakum (Hillje)	HMA	??TypeD??	Jun-07		588+1.720	594+1.773	LP 524 NORTH OF HI	0.14 MI. N. OF FM 647 (N	Y	Y	Aug-17		Unknown
94	HMA-SH 21--	HMA		Jul-09						N	N			
95	HMA-SH 21--	HMA		Jul-09						N	N			
96	HMA (better than usual material for an FM roa	HMA (better than usual r		Jul-09							N			
97	HMA-SH 71-Travis-Austin	HMA	REF	Apr-08	0265-01-103	-	-	0.6 MI W OF RIVERSID	PRESIDENTIAL DRIVE	N	Y	Jul-15	39500	Limestone/Field Sand
98	HMA-US 59-Wharton-Yoakum	HMA	REF	Sep-04	0089-08-086	560-0.090	566+0.261	FORT BEND C/L (NORTH	0.34 MI. NORTH OF SH 60	N	Y	Jun-16		NA
99	HMA-SH 154-Hopkins-Paris	HMA		May-03	0401-01-019	672+1.703	672-0.246	ROSEHILL RD	VAN ZANDT C/L	N	Y	Feb-13	7700	Sandstone

(c)

Table 17 (continued)

ID	SECTION LABEL	Surface Type	Surface Type 2	Const Date	CSJ	Proj BTRM	Proj ETRM	From	To	New	Use in query?	Confirmed Surface	AADT	Agg Type
112	HFST-SH 22-Navarro-Dallas	HFST			0121-04-026	610	NA	Curve in Blooming Grove		Y	N	Aug-17		Calcined Bauxite
113	HFST-US 287-Navarro-Dallas-A	HFST				549.8	NA			Y	N	Aug-17		Calcined Bauxite
127	HFST-FM 89-Taylor-Abilene	HFST			0699-01-049			0.127 mi S of CR 277	1.855 MI S of CR 277	Y	N			Calcined Bauxite
128	HFST-FM 2035-Nolan-Abilene	HFST			2997-01-009			0.170 MI N of CR 253	0.420 MI S of CR 253	Y	N			Calcined Bauxite
130	HFST-SH 47-Brazos-Bryan	HFST			3138-02-011	418.5	NA	Curve W of FM 60		Y	N	Aug-17		Calcined Bauxite
140	HFST-Kimbro-Travis-Austin	HFST			0914-04-293	NA	NA	OLD HWY 20	KIMBRO RD	Y	N	Aug-17		Calcined Bauxite
168	HFST-Lp 1604-Bexar-San Antonio	HFST	Bauxite and t	Late 2010		539	NA	NE I-35 at 1604 E-N connector		Y	N	Aug-17		Calcined Bauxite
174	HP Water-FM 2347-Brazos-Bryan	HP Water		Jan-11		NA		Welborn Rd	Olson Blvd		N	Nov-16	NA	
175	HP Water-SH 50-Burleson-Bryan	HP Water		Feb-11	0648-03-054	420		FM 60	SH 21	N	N	Feb-13	1400	Limestone w/ asphalt
176	HP Water-FM 455-Robertson-Bryan	HP Water		Feb-11	0262-03-029	608		SH 6 (Hearne)	Milam CL	N	N	Oct-14	2200	Lightweight (Expanded Sh
177	HP Water-US 190-Milam-Bryan	HP Water		Feb-11	0185-02, 0185-03	610		Rogers	Cameron	N	N	Nov-11	7200	Lightweight (Expanded Sh
178	HP Water-SH 90-Grimes-Bryan	HP Water		Feb-11	0315-03-051	430		FM 149	SH 6	Y	N	Aug-17	510	Lightweight (Expanded Sh
179	HP Water-FM 2562-Grimes-Bryan	HP Water		Feb-11	3302-01-013	NA		FM 149	SH 30	Y	N	Aug-17	390	Lightweight (Expanded Sh
180	HP Water-SH 321-Liberty-Beaumont	HP Water		Feb-11	0593-01-109	436		FM 1008	FM 163	N	N	NA	5800	Limestone w/ asphalt
181	HP Water-SH 63-Jasper-Beaumont	HP Water		Feb-11	0244-02-091	750		RR 255	2 mi N of RR 255	N	N	Nov-14	2800	Lightweight (Expanded Sh
182	HP Water-FM 82-Jasper-Beaumont	HP Water		Feb-11		762		US 96 (Kirbyville)	2 mi W of US 96	N	N	Nov-14	100	SAC-B
183	HP Water-FM 1472-Webb-Laredo	HP Water		Feb-11	0018-03-039	424		Toll Rd 255	RR 3338	N	N	Jan-13	19500	Limestone w/ asphalt
184	HP Water-IH 35-Webb-Laredo	HP Water		Feb-11	0018-03-043	32		MP 32	MP 33	N	N	May-14	28000	Limestone w/ asphalt
185	HP Water-FM 2950-Randall-Amarillo	HP Water		Mar-11	2614-01-017	114		FM 2219	FM 3331	N	N	Jun-13	3900	Siliceous River Gravel
186	HP Water-RM 1061-Oldham-Amarillo	HP Water		Mar-11	1245-01-012	82		FM 2381	US 385	N	N	Jan-12	1800	Siliceous River Gravel
187	HP Water-RM 294-Armstrong-Amarillo	HP Water		Feb-11	0788-03-020	108		IH 40	FM 1151	N	N	Aug-16	120	Siliceous River Gravel

(d)

APPENDIX B

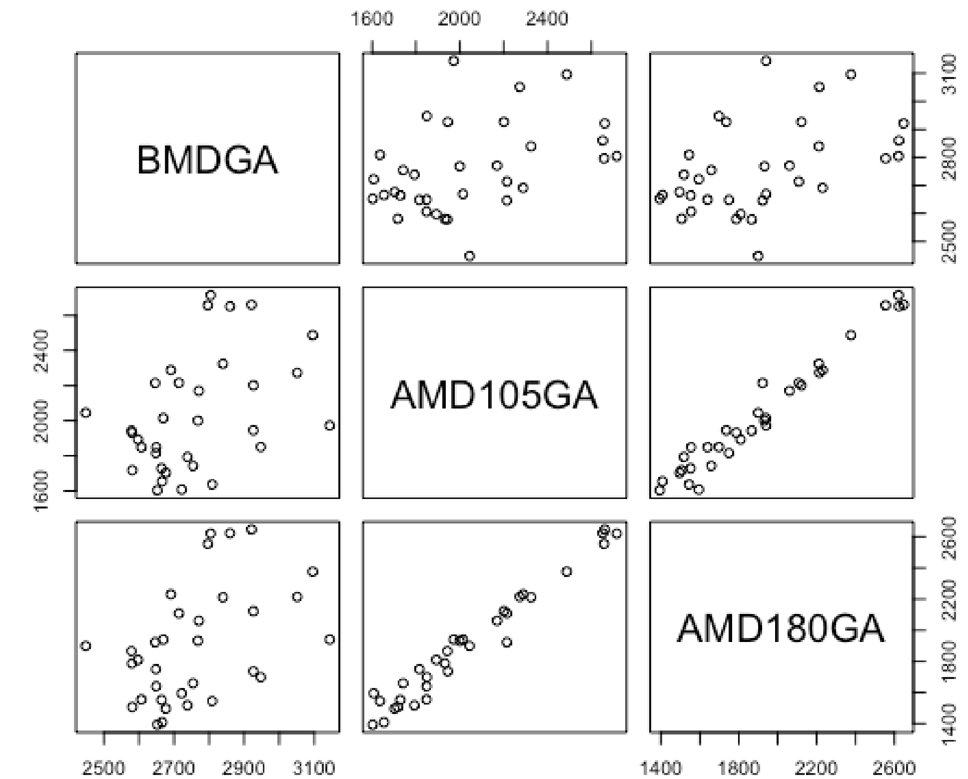

Figure 43: Plot to check relationship between angularity at different intervals

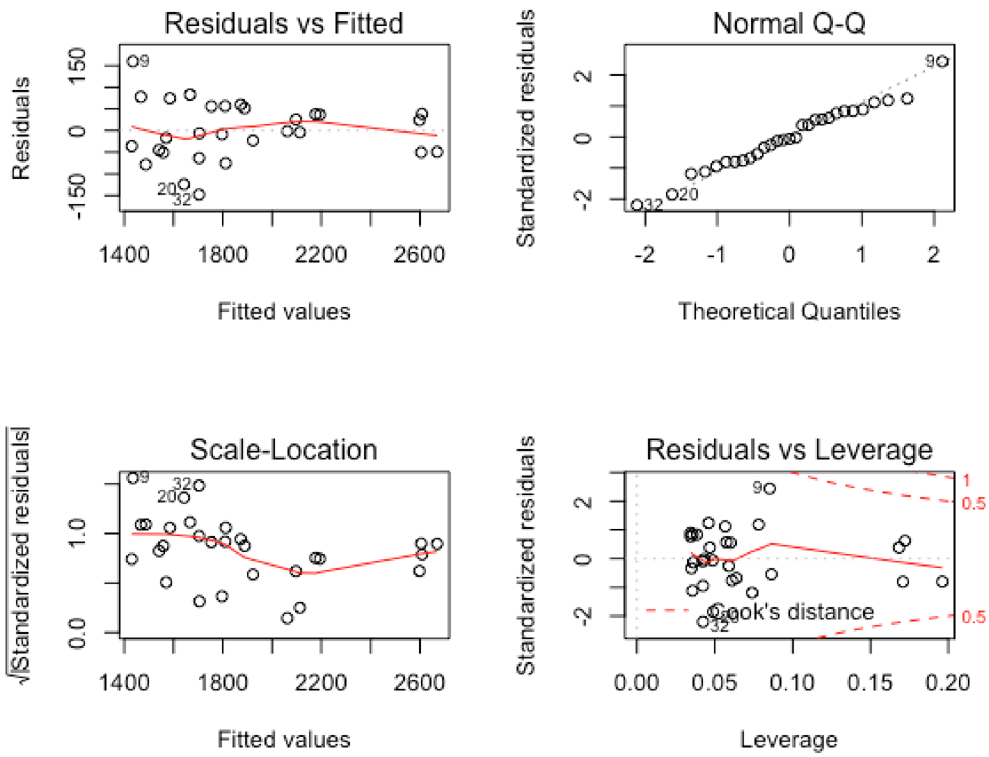

Figure 44: Diagnostic plots for angularity relationship

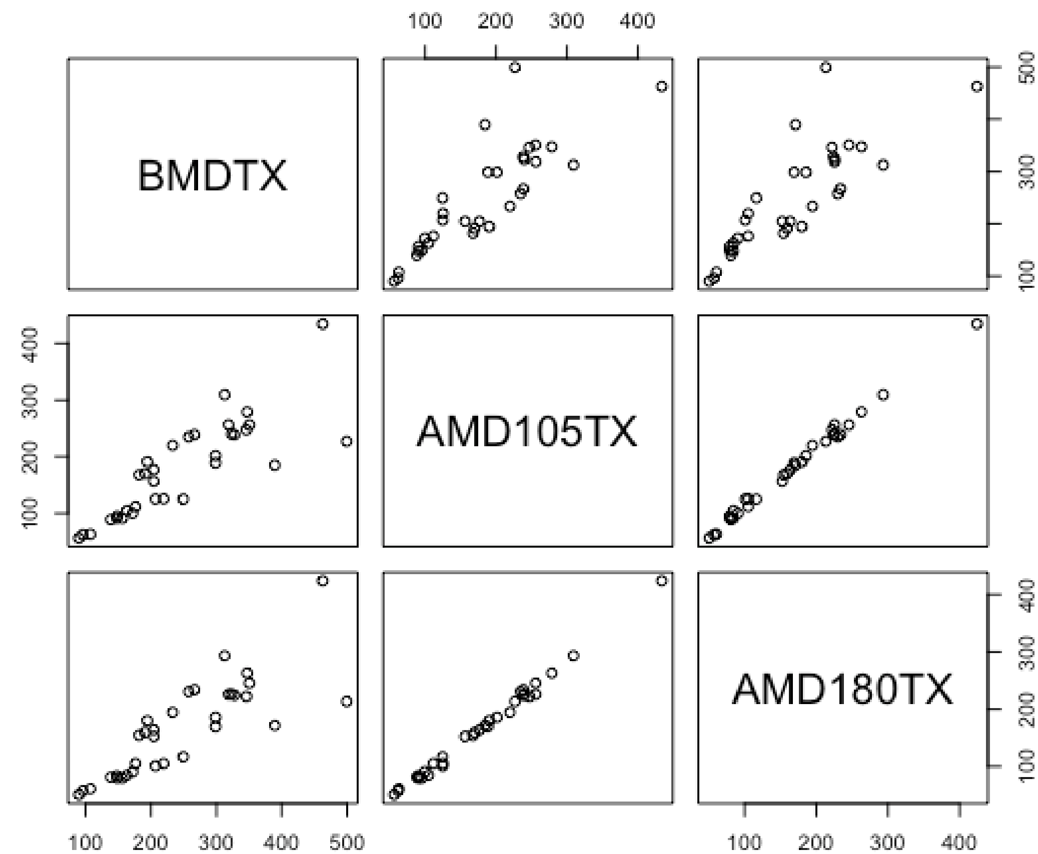

Figure 45: Plot to check relationship between texture indices at different intervals

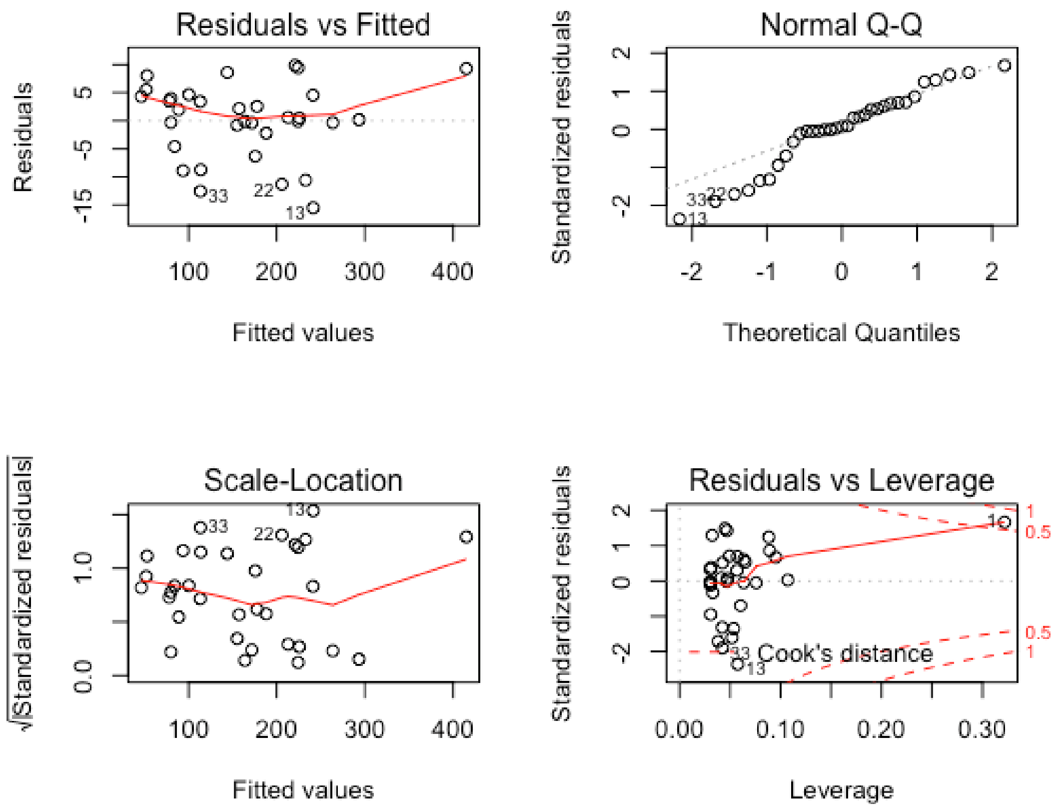

Figure 46: Plot to check relationship between texture indices at different intervals

Figure 47: Seal Coat with LWA (Streetman) Bonded with Epoxy

Figure 48: Seal Coat with LWA (Riverlite) Bonded with Epoxy

Figure 49: Seal Coat with Crushed Gravel (Phar) Bonded with Epoxy

Figure 50: Seal Coat with Limestone (TCS) Bonded with Epoxy